

DTIC FILE COPY

4

RADC-TR-89-243
Final Technical Report
November 1989

AD-A217 035



PRINCIPLES OF NONLINEAR OPTICS

Syracuse University

Partha P. Banerjee

APPROVED FOR PUBLIC RELEASE; DISTRIBUTION UNLIMITED.

DTIC
ELECTE
JAN 24 1990
S E D

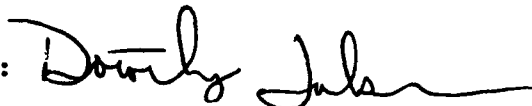
ROME AIR DEVELOPMENT CENTER
Air Force Systems Command
Griffiss Air Force Base, NY 13441-5700

90 01 23 2 28

This report has been reviewed by the RADC Public Affairs Division (PA) and is releasable to the National Technical Information Services (NTIS) At NTIS it will be releasable to the general public, including foreign nations.

RADC-TR-89-243 has been reviewed and is approved for publication.

APPROVED:



DOROTHY JACKSON
Project Engineer

APPROVED:



JOHN A. GRANIERO
Technical Director
Directorate of Communications

FOR THE COMMANDER:



BILLY G. OAKS
Directorate of Plans & Programs

If your address has changed or if you wish to be removed from the RADC mailing list, or if the addressee is no longer employed by your organization, please notify RADC (DCLW) Griffiss AFB NY 13441-5700. This will assist us in maintaining a current mailing list.

Do not return copies of this report unless contractual obligations or notices on a specific document require that it be returned.

UNCLASSIFIED

SECURITY CLASSIFICATION OF THIS PAGE

REPORT DOCUMENTATION PAGE				Form Approved OMB No. 0704-0188		
1a. REPORT SECURITY CLASSIFICATION UNCLASSIFIED			1b. RESTRICTIVE MARKINGS N/A			
2a. SECURITY CLASSIFICATION AUTHORITY N/A			3. DISTRIBUTION/AVAILABILITY OF REPORT Approved for public release; distribution unlimited.			
2b. DECLASSIFICATION/DOWNGRADING SCHEDULE N/A						
4. PERFORMING ORGANIZATION REPORT NUMBER(S) N/A			5. MONITORING ORGANIZATION REPORT NUMBER(S) RADC-TR-89-243			
6a. NAME OF PERFORMING ORGANIZATION Syracuse University		6b. OFFICE SYMBOL (If applicable)	7a. NAME OF MONITORING ORGANIZATION Rome Air Development Center (DCLW)			
6c. ADDRESS (City, State, and ZIP Code) Office of Sponsored Research Skytop Office Building, Skytop Road Syracuse NY 13210			7b. ADDRESS (City, State, and ZIP Code) Griffiss AFB NY 13441-5700			
8a. NAME OF FUNDING/SPONSORING ORGANIZATION Rome Air Development Center		8b. OFFICE SYMBOL (If applicable) DCLW	9. PROCUREMENT INSTRUMENT IDENTIFICATION NUMBER F30602-81-C-0169			
8c. ADDRESS (City, State, and ZIP Code) Griffiss AFB NY 13441-5700			10. SOURCE OF FUNDING NUMBERS			
			PROGRAM ELEMENT NO. 63726F	PROJECT NO. 2863	TASK NO. 92	WORK UNIT ACCESSION NO. PC
11. TITLE (Include Security Classification) PRINCIPLES OF NONLINEAR OPTICS						
12. PERSONAL AUTHOR(S) Partha P. Banerjee						
13a. TYPE OF REPORT Final		13b. TIME COVERED FROM Dec 87 TO Sep 88		14. DATE OF REPORT (Year, Month, Day) November 1989		
15. PAGE COUNT 100						
16. SUPPLEMENTARY NOTATION N/A						
17. COSATI CODES			18. SUBJECT TERMS (Continue on reverse if necessary and identify by block number) Optical Bistability Phase Conjugation Harmonic Generation			
FIELD	GROUP	SUB-GROUP				
20	06					
19. ABSTRACT (Continue on reverse if necessary and identify by block number) This report contains a summary of essential principles of nonlinear optics such as optical bistability, phase conjugation, and harmonic generation.						
20. DISTRIBUTION/AVAILABILITY OF ABSTRACT <input checked="" type="checkbox"/> UNCLASSIFIED/UNLIMITED <input type="checkbox"/> SAME AS RPT. <input type="checkbox"/> DTIC USERS			21. ABSTRACT SECURITY CLASSIFICATION UNCLASSIFIED			
22a. NAME OF RESPONSIBLE INDIVIDUAL Dorothy Jackson			22b. TELEPHONE (Include Area Code) (315) 330-4092		22c. OFFICE SYMBOL RADC (DCLW)	

DD Form 1473, JUN 86

Previous editions are obsolete.

SECURITY CLASSIFICATION OF THIS PAGE

UNCLASSIFIED

CONTENTS

1. Introduction	1
2. Origins of Nonlinearity	3
3. Harmonic/subharmonic Generation	11
3.1 Mathematical Formulation for One-dimensional Propagation	13
3.2 Harmonic Generation with Quadratic Nonlinearity	16
3.3 Harmonic Generation with Quadratic and Cubic Nonlinearities	24
4. Self-refraction	28
5. Optical Bistability	39
5.1 Acoustooptic Bistability	41
5.2 The Nonlinear Fabri-Perot Cavity	46
5.3 The Linear/Nonlinear Interface	61
6. Phase Conjugation	71
6.1 Comparison with Holography	74
6.2 Semiclassical Analysis	77
7. The Nonlinear Schrodinger Equation and Soliton Propagation	81
8. Conclusion	86

Accession For	
NTIS GRA&I	<input checked="" type="checkbox"/>
DTIC TAB	<input type="checkbox"/>
Unannounced	<input type="checkbox"/>
Justification	
By _____	
Distribution/	
Availability Codes	
Dist	Avail and/or Special
A-1	

1. Introduction

This presentation on nonlinear optics does not aim to be complete and detailed in the sense of recalling and accounting all experiments that were performed in the area, and carefully presenting rigorous mathematical details. Rather, it tries to present the essentials of the physics of nonlinear optics in the simplest possible way and unify all the effects under a common umbrella. What I hope to achieve is a simplified treatment of most nonlinear optical effects to provide the inexperienced reader with a springboard to jump into the sea of existing literature which is often incommensurate with respect to notations and explanations.

Without further ado, let me briefly describe the contents of this monograph. Section 2 describes the origins of nonlinearity, tracing it back to its manifestation as the modification of the linear phase velocity of a propagating wave. Relationships are established between the nonlinearity parameters we choose to use for the simplest possible description, and existing parameters (seemingly endless!) in literature. MKS units have been used consistently. Throughout the monograph, z is assumed to be the "nominal" direction of propagation and a "workhorse" dependent variable ψ used to describe the physical effect.

Section 3 is dedicated to describing the effects of harmonic/subharmonic generation. One-dimensional propagation is assumed for simplicity and the parametric interaction process involved is described. An analysis is advanced for harmonic/subharmonic generation in a quadratically nonlinear medium without any "dc" polarization, both in the presence and absence of dispersion. It is also shown that similar effects may be observed in media with quadratic and cubic nonlinearities. The very recent observation of harmonic generation in cubically nonlinear dispersive fibers has not been treated since a consolidated theory for this is still in the developmental stage.

From Section 4, we concentrate solely on effects caused by the cubic nonlinearity. In this section, for instance, we provide a simplified analysis of self-refraction of beams which occurs due to an induced refractive index profile due to the nature of the propagating beam. Not mentioned in detail is the phenomenon of "self-attraction" between adjacent beams, although a figure is devoted to illustrating the effect. More recent topics such as self-bending of an asymmetric beam in such a medium is left out for the sake of simplicity.

Another very interesting nonlinear optical effect is bistability and hysteresis, which is addressed in Section 5. To illustrate the basic principles, a hybrid acoustooptic bistable device is first considered and compared to the electronic Schmitt trigger to highlight the necessity of nonlinearity and positive feedback in achieving bistable operation. The nonlinear Fabri- Perot cavity is next analyzed using the so-called Maxwell-Bloch equations as a starting point. The limiting cases of purely absorptive and purely dispersive bistabilities are discussed in some detail. In the latter case, the onset of instability is addressed by considering familiar feedback criteria. Lastly, transmission through a linear/nonlinear interface is analyzed and bistable and hysteretic phenomena predicted. Bistable optical elements can be used as the basic building blocks of an optical computer.

The presence of a cubic nonlinearity can be sometimes exploited to achieve real-time holography or phase conjugation. This is discussed in Section 6. Principles of holography are recalled, and a semiclassical treatment of phase conjugation (also called four-wave mixing) advanced under the simplifying assumption of strong "pumps."

Finally, in Section 7, the role of a cubic nonlinearity in balancing dispersion in fibers to ensure distortionless pulse propagation is analyzed through the nonlinear Schrodinger equation, which is first heuristically derived. The distortionless pulses arising out of a balance between

nonlinearity and dispersion are commonly called solitons, and show promise of future use in fiber-optic communication systems.

While much of the discussion has been borrowed and "rebottled" in an unified way, some of the effects reported are new and the analysis novel. Reference may be made to the idea of second harmonic generation in the presence of quadratic and cubic nonlinearities, the comparison of the acoustooptic bistable device with an electronic Schmitt trigger, the treatment of purely dispersive bistability in a Fabri-Perot cavity, and the prediction of hysteresis and bistability during transmission through a linear nonlinear dispersive interface.

2. Origins of Nonlinearity

In an optically nonlinear medium, the nonlinearity can be attributed to the dependence of the phase velocity on the amplitude of the propagating wave, unlike the linear case which always assumes infinitesimal wave amplitudes. Thus, while a PDE for a wavefunction ψ of the form

$$\partial\psi/\partial t + c_0\partial\psi/\partial z = 0 \quad (1)$$

where t denotes time can explain unidirectional propagation along z in a nondispersive linear medium, the phase velocity c_0 needs to be modified to c_p according to

$$c_p = c_0(1 + \beta_2\psi + \beta_3\psi^2 + \dots) \quad (2)$$

to account for nonlinear propagation [1]. In (2), β_2 and β_3 are referred to as the quadratic and cubic nonlinearity coefficients respectively for reasons that will shortly become clear. The wavefunction, ψ may represent a component of the (real) electric field.

In the nonlinear regime, eq. (1) is modified, in the light of (2), to

$$\partial\psi/\partial t + c_0(1 + \beta_2\psi + \beta_3\psi^2)\partial\psi/\partial z = 0 \quad (3a)$$

or

$$\partial\psi/\partial t + c_0\partial\psi/\partial z + (c_0\beta_2/2)\partial\psi^2/\partial z + (c_0\beta_3/3)\partial\psi^3/\partial z = 0, \quad (3b)$$

justifying the names given to β_2 and β_3 above. We remark that the nonlinearity, e.g., β_2 , is responsible for shock formation during fluid flow due to steepening of the (baseband) wavefronts as shown in fig. 1. This happens since the parts of the baseband pulse having larger amplitudes travel faster than the parts with smaller amplitudes for $\beta_2 > 0$, leading to a point in time where the right edge of the pulse develops infinite steepness or 'shock.' In optics, the quadratic nonlinearity (and cubic nonlinearity, too!) is responsible for second harmonic/subharmonic generation, and this will be discussed in Section 3. Special effects arising from the cubic nonlinearity will be mentioned below and discussed at length in sections 4 - 7.

The reader may realize that the simple model described above cannot describe wave propagation in higher dimensions, necessitating the need for a higher order PDE. This can be readily derived from (3) by differentiating w.r.t. t and reusing (3) to simplify. This yields, after some algebra,

$$\partial^2\psi/\partial t^2 - c_0^2\partial^2\psi/\partial z^2 \approx 2c_0^2 [(\beta_2/2)\partial^2\psi^2/\partial z^2 + (\beta_3/3)\partial^2\psi^3/\partial z^2] \quad (4a)$$

$$\approx \beta_2\partial^2\psi^2/\partial t^2 + (2\beta_3/3)\partial^2\psi^3/\partial t^2 \quad (4b)$$

under the assumption of weak nonlinearity [2]. This assumption helps us neglect second-order terms in $\beta_{2,3}$ in deriving (4a), and in approximating

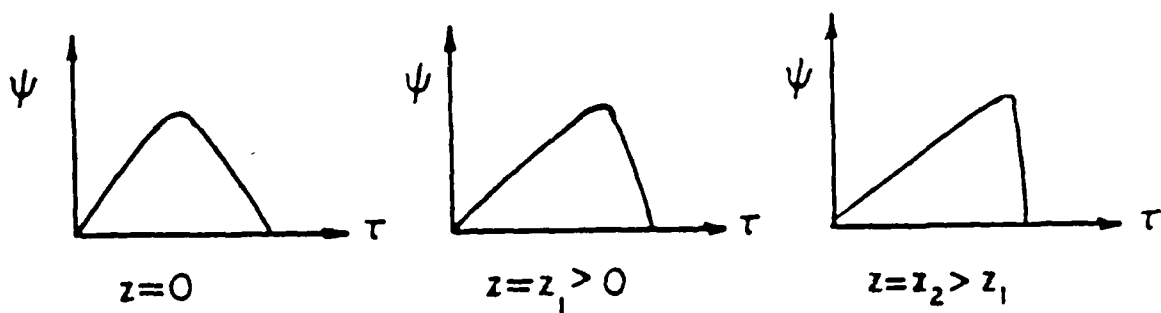


Fig. 1. Evolution of shock during propagation of a baseband pulse. The nonlinearity parameter χ_2 is assumed to be positive. $\tau = t - z/c_0$ is a moving frame of reference.

$\partial^2/\partial z^2$ by $c_0^{-2} \partial^2/\partial t^2$ on the RHS of (4a) in deriving (4b). The extension to higher dimensions may be effectively done by replacing $\partial^2/\partial z^2$ in (4b) by the Laplacian ∇^2 :

$$\partial^2 \psi / \partial t^2 - c_0^2 \nabla^2 \psi \approx \beta_2 \partial^2 \psi^2 / \partial t^2 + (2\beta_3/3) \partial^2 \psi^3 / \partial t^2. \quad (5)$$

As will become clear later in this section, eq. (5) with $\beta_{2,3} \neq 0$ becomes the wave equation for a component of the \vec{E} field where the RHS may be identified to be the source term due to the nonlinear polarization of the medium. While the quadratically nonlinear induced polarization is responsible for second harmonic/subharmonic generation as stated earlier, the cubically nonlinear induced polarization gives rise to an amplitude-dependent refractive index which causes self-refraction, and can account for other nonlinear optical effects such as bistability, phase-conjugation, soliton propagation etc., to be discussed later.

At this point, it is instructive to strike a connection between the nonlinearity parameters β_2, β_3 introduced above and the commonly occurring parameters in nonlinear optics literature. There, the description of nonlinearities is given in terms of the nonlinear induced polarization in the medium or an amplitude dependent refractive index. In the former, the induced polarization P_i is expressed in terms of a Taylor series expansion of the electric field component E_j according to [3]

$$P_i = \epsilon_0 \chi_{ij} E_j + \epsilon_0 \chi_{ijk} E_j E_k + \epsilon_0 \chi_{ijkl} E_j E_k E_l + \dots \quad (6a)$$

$$\Delta \epsilon_0 \chi_{ij} E_j + 2d_{ijk} E_j E_k + \epsilon_0 \chi_{ijkl} E_j E_k E_l \quad (6b)$$

$$\Delta \epsilon_0 \chi_{ij} E_j + P_i^{NL} \quad (6c)$$

where the Einstein convention for summation over repeated indices has been employed. In (6), χ_{ij} is the linear susceptibility, while χ_{ijk} and χ_{ijkl} refer to the second and third-order nonlinear optical susceptibilities respectively. The reader, not quite familiar with tensor notation, has scope for being baffled for sometime at first, but may take heart from the fact that (6) is merely a shorthand for writing lengthy expressions. For example, without the last two terms of the RHS of (6), P_1 , the x-component of the polarization may be expressed as

$$P_1 = \epsilon_0 (\chi_{11} E_1 + \chi_{12} E_2 + \chi_{13} E_3) \quad (7)$$

where E_1, E_2, E_3 stand for the x, y and z components of the electric field in a medium where, in general, $\chi_{11} \neq \chi_{12} \neq \chi_{13}$, if the medium is anisotropic. Readers may be reassured that the new representation is not usually necessary to explain the nonlinear effects mentioned earlier, but should be familiar with it in case of cross-referencing with existing literature.

The wave equation for the vector electric field \vec{E} may be readily derived from Maxwell's equations by writing

$$\vec{D} = \epsilon_0 \vec{E} + \vec{P} \quad (8)$$

where the components of \vec{P} are specified in (6). This yields

$$\partial^2 \vec{E} / \partial t^2 - c_0^2 \nabla^2 \vec{E} = - (\mu_0 / \epsilon) \partial^2 \vec{P}^{NL} / \partial t^2 \quad (9)$$

in a region free of sources and currents and for a medium which is isotropic in the linear regime ($\chi_{ij} = \chi_L$). In (9),

$$\epsilon = \epsilon_0 (1 + \chi_L) \quad (10a)$$

and

$$c_o = (1/\mu_o \epsilon)^{1/2}. \quad (10b)$$

It is true that through eq. (9), one can obtain a set of coupled PDEs, in general, that describes the behavior of a certain component of the electric field. However, as will be shown later, similar equations may also be derived by starting from (5) and assuming no particular anisotropy in the medium. To explain the physics of what is happening, we shall therefore use eqns. (3) or (5) as our starting point.

To obtain typical values for β_2 , for instance, note that a comparison of (4b) and (9), with (6), shows that β_2 is of the order of $-2(\mu_o/\epsilon)d_{ijk} = -2\mu_o \epsilon_o (1 + \chi_L)d_{ijk}$. Listed below are some typical values for d_{ijk} along with the corresponding wavelengths at which they are measured [3]:

crystal	$\lambda(\mu m)$	$d_{ijk} \left(\frac{1}{9} \times 10^{-22} \text{ m}^3/\text{V-s}^2 \right)$
GaAs	10.6	$d_{123} : 107$
InSb	28	$d_{123} : 462$
CdTe	28	$d_{123} : 48$
CdS	10.6	$d_{333} : 35$
		$d_{311} : -21$
	1.06	$d_{333} : 80$
LiNbO ₃	1.06	$d_{333} : -27$
		$d_{222} : 4$
quartz	1.064	$d_{111} : 0.4$
KDP	0.6328	$d_{213} : 0.57$
	1.06	$d_{312} : 0.50$

Table 1. Quadratic nonlinearity coefficients d_{ijk} for some crystals.

We caution readers that the values of d_{ijk} in Table 1 are only valid for the case of second harmonic generation. For the general three-frequency interaction case ($\omega_3 = \omega_1 + \omega_2$), the values of d_{ijk} may be different than those listed.

Now to prescribe typical values for β_3 , the cubic nonlinearity coefficient, we will first state its relationship with the amplitude-dependent refractive index coefficient n_2 defined as [3]

$$n = n_0 + (1/2)n_2\psi_e\psi_e^* \quad (11)$$

where ψ_e represents the envelope of ψ : $\psi = \text{Re} \{ \psi_e \exp j(\omega_0 t - k_0 z) \}$, and where n_0 denotes the linear refractive index. This can be readily achieved by starting from (2) with $\beta_2 = 0$ and invoking the weak nonlinearity assumption. The result is

$$\beta_3 = -2n_2/n_0. \quad (12)$$

The units of n_2 and β_3 are m^2/V^2 in MKS since ψ_e has units of V/m. We specifically point this out for the benefit of readers who, like us, will no doubt be frustrated at different unit systems that are used in literature, as well as different definitions of the nonlinear polarization and the nonlinear refractive index coefficient. For instance, an equivalent representation of the nonlinear refractive index that appears in literature is [4]

$$n = n_0 + \gamma I, \quad (13)$$

where I is the optical intensity or irradiance. γ has the unit of m^2/W and is related to n_2 as

$$\gamma = n_2 / c \epsilon_0 n_0. \quad (14)$$

Finally, n_2 is related to a nonlinear susceptibility viz. χ_{1111} as

$$n_2 = 3\chi_{1111}/n_0, \quad (15)$$

for the case of an electric field linearly polarized in, say, the x-direction. Eq. (15) may be derived by writing E and P^{NL} in (9) in terms of their slowly varying envelopes E_e and P_e^{NL} , setting $P_e^{NL} = 3\epsilon_0\chi_{1111}E_e^2E_e^*$ (see (6b)) and finding the effective propagation constant. The factor 3 above is a degeneracy factor which arises in the interaction process $\omega_0 = \omega_0 + \omega_0 - \omega_0$. Values of χ_{1111} for different materials are listed in Table 2 [5].

Material	$\lambda (\mu m)$	n_0	$\chi_{1111} (\frac{4\pi}{9} \times 10^{-21} m^2/V^2)$
GaAs	10.6	3.3	120
InSb	5.3	4	-6×10^{10}
	10.6	4	2×10^6
CdTe	1.06	3	2.5×10^5
CdS	0.694	2.42	130
Ge	10.6	4	10^3
Si	10.6	3.4	60
H ₂ O	0.694	1.33	0.7
Acetone	0.694	1.35	1.8
Benzene	1.064	1.5	2.4

Table 2. Cubic nonlinearity coefficients χ_{1111} for some materials.

3. Harmonic/Subharmonic Generation

An important consequence of nonlinearity is frequency multiplication. To see what this means consider, first, one dimensional CW propagation in a quadratically nonlinear ($\beta_2 \neq 0$, $\beta_3 = 0$) nondispersive medium. If a CW wave of angular frequency ω and propagation constant k is incident on such a medium, it can generate harmonics that travel along with the same velocity. The energy and momentum conservation laws as well as the dispersion relationship (variation of ω with k) have to be satisfied whenever wave interactions occur [6]. Limiting ourselves to only two frequencies, namely the fundamental (ω_0 , k_0) and the second harmonic ($2\omega_0$, $2k_0$), the following interaction occurs:

$$\omega_0 + \omega_0 \rightarrow 2\omega_0 ; 2\omega_0 - \omega_0 \rightarrow \omega_0$$

$$k_0 + k_0 \rightarrow 2k_0 ; 2k_0 - k_0 \rightarrow k_0$$

with $\omega_0/k_0 = c_0$, the phase velocity of the two propagating frequencies. The relation (15) depicts explicitly, for example, the parametric mixing of two waves at (ω_0, k_0) through a quadratic nonlinearity to yield a third wave at $(2\omega_0, 2k_0)$. This is the basis of second harmonic generation usually observed in nonlinear electrooptic crystals [3], [4], [7].

The next question to ask is: Could a cubic nonlinearity also play a role in second harmonic generation? At first thought, this seems doubtful, since a cubic nonlinearity can only facilitate interactions of the type $\omega_0 + \omega_0 + \omega_0 \rightarrow 3\omega_0$ leading to third harmonic generation. A closer examination has revealed, however, that the answer is yes, but only if either the quadratic nonlinearity is also present, or if a "dc" source of energy is either externally applied or internally generated [8]. The latter case is in support of recent observations of second harmonic generation in optical

fibers which can only have odd-order nonlinearities. We will not treat this case since, at this time, no undisputed explanation is available. In the former case, the parametric mixing that occurs can be represented as:

$$\begin{aligned}
 2\omega_0 + \omega_0 - \omega_0 &\rightarrow 2\omega_0, \quad 2\omega_0 - 2\omega_0 + 2\omega_0 \rightarrow 2\omega_0; \\
 \omega_0 + 2\omega_0 - 2\omega_0 &\rightarrow \omega_0, \quad \omega_0 - \omega_0 + \omega_0 \rightarrow \omega_0,
 \end{aligned}
 \tag{17}$$

with similar relations for the k 's. The parametric process described above may be visualized as contributions to the growth of the second harmonic amplitude in the presence of the fundamental (and vice-versa).

If, now, the medium under consideration is dispersive, the propagation constants for the frequencies ω_0 and $2\omega_0$ are no longer related by a simple factor (viz., $k_2 \stackrel{\Delta}{=} k(2\omega_0) = 2k_1 \stackrel{\Delta}{=} k(\omega_0)$). For one-dimensional propagation, this gives rise to a spatial beating for the fundamental and harmonic (subharmonic) amplitudes, which in the general theory of nonlinear waves, is called the "Fermi-Pasta-Ulam" recurrence phenomenon [9]. The recurrence period, which in the linear case for two propagating frequencies is given by $2\pi/(k_2 - 2k_1)$, is modified by the presence of nonlinearities, to be explained in detail below.

In many physical situations, however, wave propagation is essentially higher-dimensional unless special care is taken to ensure one-dimensional propagation. For the higher-dimensional dispersive case, the two frequencies are no longer constrained to propagate in the same direction, and hence interact according to the "resonant-triad" relations [6]

$$\begin{aligned}
 \omega_1 + \omega_2 &\rightarrow \omega_3 \\
 \bar{k}_1 + \bar{k}_2 &\rightarrow \bar{k}_3
 \end{aligned}
 \tag{18a}$$

with

$$\omega_1 = \omega(|\bar{k}_1|). \quad (18b)$$

The resonance triad vector diagram is shown in fig. 2 for the case $\omega_1 = \omega_2 = \omega_0$ and $\omega_3 = 2\omega_0$. Since the waves are "free" to travel in higher dimensions (predictable from the vector diagram and the dispersion relationship), there is no longer any spatial beating due to dispersion, and the evolution of the second harmonic/subharmonic is similar to the nondispersive case, albeit in their respective directions [6], [10], [11]. The rigorous mathematical formulation of this case is beyond the scope of this discussion.

3.1 Mathematical Formulation for One-dimensional Propagation

We first assume $\psi(z,t)$ to be representable as

$$\psi(z,t) = \frac{1}{2} \sum_{n=-2}^2 \Psi_n(z) \exp [jn(\omega_0 t - k_0 z)] \quad (19)$$

with $\Psi_0 = 0$ (no dc component); and with $\Psi_{-n} = \Psi_n^*$ to ensure that the wavefunction is real. Then substituting (19) into (3) and gathering terms around the respective frequency components, viz., ω_0 and $2\omega_0$, we obtain the following set of coupled spectral evolution equations [8]:

$$\begin{aligned} d\Psi_n/dz = & (jk_0\beta_2/2) \sum_{m=-2}^2 m\Psi_m \Psi_{n-m} \\ & + (jk_0\beta_3/4) \sum_{m=-2}^2 \sum_{\ell=-2}^2 \ell\Psi_\ell \Psi_{m-\ell} \Psi_{n-m}. \end{aligned} \quad (20)$$

In deriving (20), we have assumed $\omega_0/k_0 = c_0$ and that $\Psi_n(z)$ is a slowly

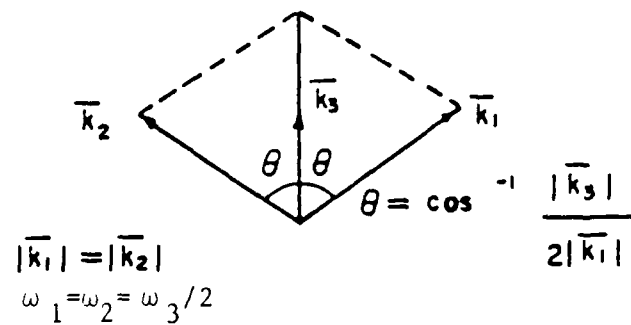


Fig. 2. Resonant triad wavevector diagram for three interacting waves 1, 2 and 3, two of which have the same temporal frequency. The wavevector diagram follows from the conservation of momentum during wave interactions and the dispersion characteristics of the system. The interaction angle θ depends on the amount of dispersion.

varying function of z in the sense that $|d\Psi_n/dz| \ll |nk_0\Psi_n|$. Note that the first and second terms on the RHS of (20) respectively denote the contributions from the quadratic and cubic nonlinearities.

To account for the effect of dispersion, we must slightly modify (20). To do this, we may realize that in the presence of dispersion alone, the propagation constant for the ' n '-th harmonic can be written as k_n . Thus, during propagation, the spatial behavior of Ψ_n will be [12]

$$\Psi_n = \Psi_n(0) \exp[-j(k_n - nk_0)z], \quad (21)$$

so that in (19),

$$\Psi(z,t) = (1/2) \sum_{n=-2}^2 \Psi_n(0) \exp[j(n\omega_0 t - k_n z)], \quad (22)$$

as expected. Now (21) is analogous to

$$d\Psi_n/dz = -j(k_n - nk_0)\Psi_n. \quad (23)$$

To incorporate the effect of dispersion in our nonlinear system (20), we may heuristically add a term as on the RHS of (23) to the RHS of (20) if the nonlinear and dispersive effects are small:

$$\begin{aligned} d\Psi_n/dz = & (jk_0\beta_2/2) \sum_{m=-2}^2 m\Psi_m \Psi_{n-m} \\ & + (jk_0\beta_3/4) \sum_{m=-2}^2 \sum_{\ell=-2}^2 \ell\Psi_\ell \Psi_{m-\ell} \Psi_{n-m} \\ & - j(k_n - nk_0)\Psi_n. \end{aligned} \quad (24)$$

Eq. (24) will serve as our model equation describing the evolution of the fundamental and the second harmonic in a medium with quadratic and cubic nonlinearities, and dispersion. In what follows, we will consider two special cases: (a) harmonic generation with quadratic nonlinearity without and with dispersion, and (b) harmonic generation with quadratic and cubic nonlinearities and no dispersion. Comments on subharmonic generation will also be made.

3.2 Harmonic Generation with Quadratic Nonlinearity

In this case, with $\beta_2 \neq 0$, $\beta_3 = 0$, eq. (24) gives the following set of equations for $n = 1$ and 2:

$$d\Psi_1/dz = j(\beta_2 k_0/2)\Psi_1\Psi_2 - j(k_1 - k_0)\Psi_1, \quad (25a)$$

$$d\Psi_2/dz = j(\beta_2 k_0/2)\Psi_1^2 - j(k_2 - 2k_0)\Psi_2, \quad (25b)$$

where Ψ_1 , Ψ_2 denote the complex spectral amplitudes at ω_0 and $2\omega_0$. Note that we have retained the symbols k_1 and k_2 to stand for the propagation constants at the frequencies ω_0 and $2\omega_0$ respectively at this point. In principle, k_1 could be set equal to k_0 without loss of generality; however, we choose to retain the distinction to bring out the effect of dispersion more succinctly. We will now resolve the complex spectral amplitudes into their respective (real) amplitudes and phase by writing

$$\Psi_n = a_n \exp[-j\phi_n] = \Psi_{-n}^* \quad (26)$$

in (25). This yields the following set of four equations:

$$da_1/dz = (\beta_2 k_0/2) a_1 a_2 \sin(\phi_2 - 2\phi_1), \quad (27a)$$

$$da_2/dz = -(\beta_2 k_0/2) a_1^2 \sin(\phi_2 - 2\phi_1), \quad (27b)$$

$$d\phi_1/dz = -(\beta_2 k_0/2) a_2 \cos(\phi_2 - 2\phi_1) + (k_1 - k_0), \quad (28a)$$

$$d\phi_2/dz = -(\beta_2 k_0/2) (a_1^2/a_2) \cos(\phi_2 - 2\phi_1) + (k_2 - 2k_0). \quad (28b)$$

Now, (28a,b) can be combined by defining

$$\theta \triangleq \phi_2 - 2\phi_1 \quad (29)$$

to give

$$d\theta/dz = \Delta k + (\beta_2 k_0/2) (2a_2 - a_1^2/a_2) \cos \theta, \quad (30)$$

where

$$\Delta k \triangleq k_2 - 2k_1 \quad (31)$$

is proportional to what is often called the "phase velocity mismatch" due to dispersion. Remark that from (27a,b), it readily follows that

$$a_1^2 + a_2^2 = \text{constant} = a_1^2(0) + a_2^2(0) = \tilde{E}, \quad (32)$$

depicting conservation of energy. Finally, normalization using the definitions

$$\begin{aligned}\xi &= (\beta_2 k_0/2) \bar{E}^{1/2} z, \\ \Delta s &= 2\Delta k/(\beta k_0 \bar{E}^{1/2}),\end{aligned}\tag{33}$$

$$u = a_1/\bar{E}^{1/2},$$

$$v = a_2/\bar{E}^{1/2}$$

reduces the system (27), (32) to

$$du/d\xi = uv \sin \theta,\tag{34a}$$

$$dv/d\xi = -u^2 \sin \theta,\tag{34b}$$

$$d\theta/d\xi = \Delta s + (2v-u^2/v) \sin \theta,\tag{35}$$

where we have used the definition of θ as in (29). Observe, also, that using (34a,b),

$$\begin{aligned}d[\ln(u^2 v)]/d\xi &= (2/u) du/d\xi + (1/v) dv/d\xi \\ &= (2v-u^2/v) \sin \theta;\end{aligned}\tag{36}$$

hence, (35) may be recast in the form

$$d\theta/d\xi = \Delta s + \cot \theta \, d[\ln(u^2 v)]/d\xi.\tag{37}$$

Eqs. (34), (37) therefore describe the evolution of the real amplitudes and

the relative phase difference during propagation in a quadratically nonlinear dispersive medium [7], [13].

Consider, first, the case when $\Delta s = 0$ (perfect phase-matching). Then, from (37), one integration yields

$$u^2 v \cos \theta = \text{constant} \stackrel{\Delta}{=} \Gamma = u^2(0) v(0) \cos \theta(0). \quad (38)$$

Now, using (34b), (38) and realizing that

$$u^2 + v^2 = 1, \quad (39)$$

we can write

$$d(v^2)/d\xi = \mp 2v(1-v^2) [1 - \Gamma^2/v^2(1-v^2)^2]^{1/2}$$

or

$$\xi = \pm (1/2) \int_{v^2(0)}^{v^2(\xi)} [v^2(1-v^2)^2 - \Gamma^2]^{-1/2} d(v^2). \quad (40)$$

The general solution to $v(\xi)$ (and hence to $u(\xi)$ and $\theta(\xi)$), as given by (40), is rather complicated if $v(0) \neq 0$. Suffice here to state that the solution depends on the roots of the equation

$$v^2(1-v^2)^2 - \Gamma^2 = 0 \quad (41)$$

which may, for now, be written as v_a^2 , v_b^2 and v_c^2 , with

$$v_c^2 \geq v_b^2 \geq v_a^2. \quad (42)$$

The solution is expressible in terms of Jacobian elliptic functions like

'cn' and 'sn' which look similar to the 'cos' and 'sin' functions, and are periodic in nature, with a period Π_ξ given as [14]

$$\Pi_\xi = \int_{v_a^2}^{v_b^2} [v^2(1-v^2)^2 - \Gamma^2]^{-1/2} d(v^2). \quad (43)$$

A case of physical interest is where $v(0) = 0$ ($u(0) \neq 0$), i.e., when we want to generate the second harmonic starting from the fundamental. Then $\Gamma = 0$ (from (38)) and $v_a^2 = 0$, $v_b^2 = v_c^2 = 1$ (from (42)). The period Π_ξ (using (43)) becomes infinity. (40) may be readily integrated to give

$$v(\xi) = \tanh \xi \quad (44)$$

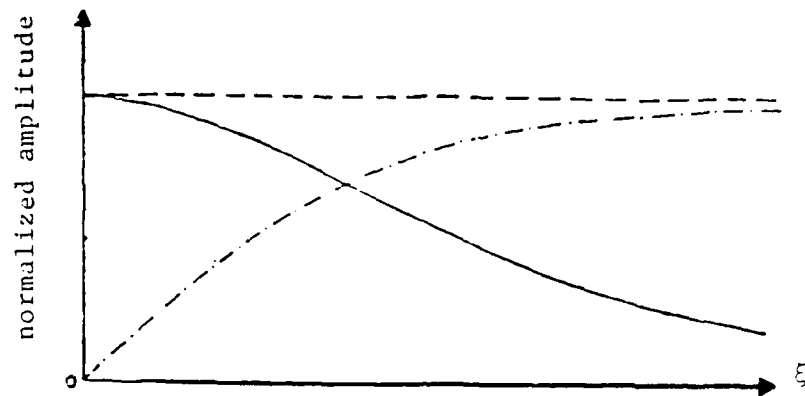
so that from (39), a possible solution to u is

$$u(\xi) = \operatorname{sech} \xi. \quad (45)$$

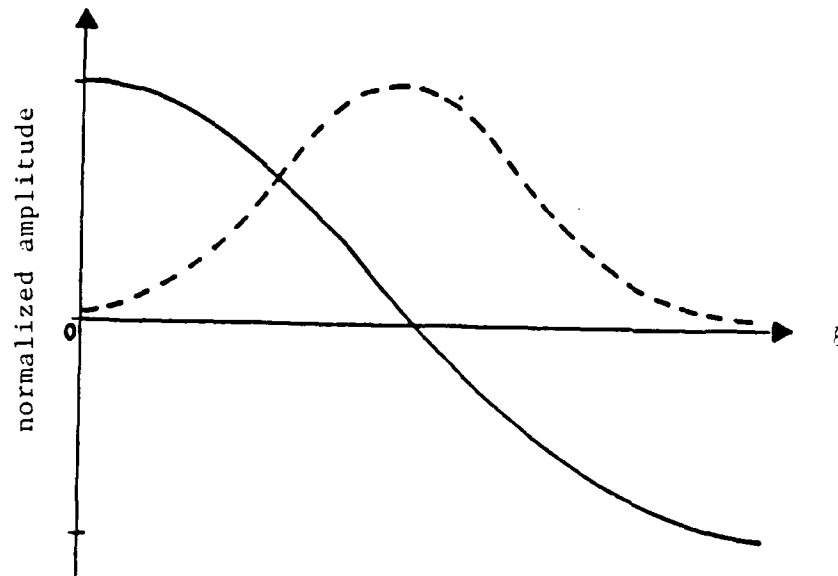
Now, (44), (45) suggest that at $\xi = 0$, $\theta(0) = -\pi/2$ (using (34)) = $\theta(\xi)$ (using (35)) since $\Delta s = 0$ (perfect phase matching). A plot of u and v is shown in fig. 3a. Note that the fundamental amplitude asymptotically goes to zero; while the second harmonic amplitude asymptotically tends to 1, although in a physical system with attenuation, the second harmonic amplitude eventually decays to zero.

We remark, in passing, that eqs. (34), (35) may also be used to explain subharmonic generation. For this, we have to take $v(0) \neq 0$, and assume a small amount of the subharmonic (u) exists in the system due to ambient noise. If we assume this initial amount of the subharmonic ($=\epsilon v(0)$), it is easy to check that for $\theta(0) = \pi/2$, the solution to (34) may be expressed as

$$u(\xi) = \operatorname{sech} (\xi - \xi_0), \quad (46a)$$



(a)



(b)

Fig. 3. Theoretically predicted variation of (a) fundamental — and second harmonic -.-.- amplitudes and (b) fundamental — and subharmonic --- amplitudes due to quadratic nonlinearity and in the case of perfect phase matching. While the second harmonic grows from zero, the subharmonic is amplified from noise level.

$$v(\xi) = -\tanh(\xi - \xi_0), \quad (46b)$$

with

$$\xi_0 = \tanh^{-1} v(0) \approx (1/v(0)) \ln(1/\varepsilon) \quad (47)$$

and where

$$v^2(0)(1+\varepsilon^2) = 1, \quad (48)$$

to ensure conservation of energy. A plot of u and v for this case is shown in fig. 3b.

Consider, next, the case when $\Delta s \neq 0$ (imperfect phase-matching). In this case, multiplying (35) with $u^2 v \sin \theta$ and using (34), we get [7], [13]

$$(d/d\xi)[u^2 v \cos \theta] + (\Delta s/2) d(v^2)/d\xi = 0. \quad (49)$$

Integration gives

$$\begin{aligned} u^2 v \cos \theta + (\Delta s/2) v^2 &= \text{constant} \stackrel{\Delta}{=} \Gamma_{\Delta s} \\ &= \Gamma + (\Delta s/2) v^2(0). \end{aligned} \quad (50)$$

Eq. (40) is now generalized as

$$\xi = \pm (1/2) \int_{v^2(0)}^{v^2(\xi)} [v^2(1-v^2)^2 - \{\Gamma - (\Delta s/2)(v^2 - v^2(0))\}^2]^{-1/2} d(v^2). \quad (51)$$

Everything previously said about (40) and its solutions for $v(0) \neq 0$ carries

over to the solution of (51), and the period in this case is given by

$$\Pi_{\xi} = \int_{v_a^2}^{v_b^2} [v^2(1-v^2)^2 - \{\Gamma - (\Delta s/2)(v^2 - v^2(0))\}^2]^{-1/2} d(v^2), \quad (52)$$

where v_c^2, v_b^2, v_a^2 (with $v_c^2 \geq v_b^2 \geq v_a^2$) denotes the roots of the quantity in square brackets in the above expression.

As before, a case of physical interest is where $v(0) = 0$ ($u(0) \neq 0$). We will find the period of oscillation for this case. To do this, we recast (52) into the form

$$\Pi_{\xi} = (2/v_c) \int_0^{\pi/2} d\alpha [1 - (v_b/v_c)^2 \sin^2 \alpha]^{-1/2} \quad (53)$$

by employing the substitution

$$\sin^2 \alpha = (v^2 - v_a^2) / (v_b^2 - v_a^2) \quad (54)$$

and noting that for $v(0) = 0$, $\Gamma = 0$ and $v_a = 0$. The other two roots are given by the solution to the algebraic equation

$$v^2(1-v^2)^2 - \{(\Delta s/2)v^2\}^2 = 0 \quad (55)$$

as

$$v_c^2 = [\Delta s/4 + \{1 + (\Delta s/4)^2\}^{1/2}]^2 = 1/v_b^2. \quad (56)$$

For the severely mismatched case ($\Delta s \gg 1$), it can be shown, after simple algebra, that

$$v_b^2 \approx (2/\Delta s)^2 [1 - 8/(\Delta s)^2] \quad (57a)$$

$$v_c^2 \approx (\Delta s/2)^2 [1 + 2/(\Delta s)^2], \quad (57b)$$

so that (53) straightforwardly yields (using (8.57))

$$\Pi_\xi = (2\pi/\Delta s) (1 - 4/(\Delta s)^2). \quad (58)$$

[The period in z may be readily found using the transformations in (33)]. The growth of the second harmonic amplitude for different values of phase mismatch is shown in fig. 4. In the theory of nonlinear waves, this periodic behavior is referred to as the Fermi-Pasta-Ulam (FPU) recurrence [9].

3.3 Harmonic Generation with Quadratic and Cubic Nonlinearities

We will discuss, in this section, the problem of harmonic generation with quadratic and cubic nonlinearities, and no dispersion. The case with dispersion follows in a similar way, and will not be discussed here, since our intention is to simply point out the criteria that dictate harmonic generation in a quadratically and cubically nonlinear environment.

For the analysis, we return to eq. (24), and neglect dispersion to write down the following set of equations for the spectral amplitudes Ψ_1 and Ψ_2 [8]:

$$d\Psi_1/dz = j(k_0\beta_2/2) \Psi_{-1}\Psi_2 + j(k_0\beta_3/4) (\Psi_{-1}\Psi_1^2 + 2\Psi_1\Psi_2\Psi_{-2}) \quad (59a)$$

$$d\Psi_2/dz = j(k_0\beta_2/2) \Psi_1^2 + j(k_0\beta_3/2) (\Psi_2^2\Psi_{-2} + \Psi_1\Psi_{-1}\Psi_2). \quad (59b)$$

Now, using the same procedures as that followed in Section 3.2, we can

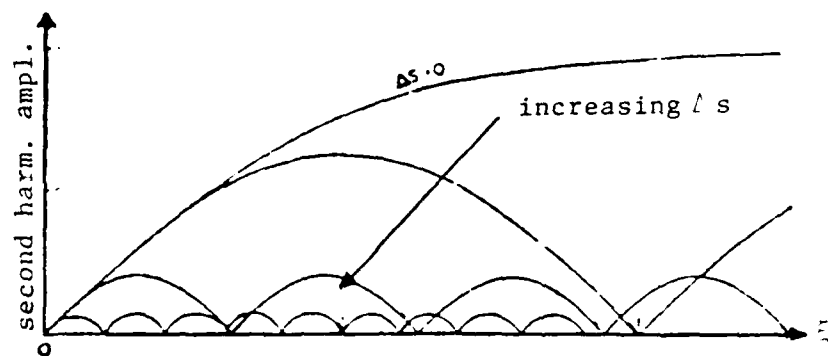


Fig. 4. Growth of the second harmonic amplitude with propagation in the phase-mismatched case. For comparison, the phase-matched case is included in the figure. The approximate expression for the period is given in eq. (58).

derive the coupled equations between the (normalized) real amplitudes and the relative phase difference. Relations to use are (26), (29), (32) and (33) without the phase mismatch term Δs , and the definition

$$\bar{Q} = (\beta_3/2\beta_2) \bar{E}^{1/2}. \quad (60)$$

The quantity \bar{Q} may be thought of as a parameter describing the ratio of the cubic and quadratic nonlinearity coefficients. The set of coupled equations for this case eventually becomes

$$du/d\xi = uv \sin \theta, \quad (61a)$$

$$dv/d\xi = -u^2 \sin \theta \quad (61b)$$

and

$$d\theta/d\xi = 2\bar{Q}(v^2 - u^2) + (2v - u^2/v) \cos \theta. \quad (62)$$

As expected, eqs. (61), (62) for $\bar{Q} = 0$ (no cubic nonlinearity) become identical to eqs. (34), (35) for $\Delta s = 0$ (no dispersion).

To solve the above system, we proceed analogous to the method in section (3.2) for $\Delta s \neq 0$. For instance, multiplying (62) by $u^2 v \sin \theta$ and using (61) to simplify, we get, after some algebra,

$$u^2 v \cos \theta = \bar{Q} u^2 v^2 = \text{constant} \stackrel{\Delta}{=} \Gamma_0 = u^2(0) v(0) \cos \theta(0) + \bar{Q} u^2(0) v^2(0). \quad (63)$$

Finally, using (61b), (39) and (63), and integrating, we obtain

$$\xi = \pm(1/2) \int_{v^2(0)}^{v^2(\xi)} [v^2(1-v^2)^2 - \{\Gamma_0 - \tilde{Q}(1-v^2)v^2\}^2]^{-1/2} d(v^2). \quad (64)$$

The quantity in square brackets, unlike the similar expressions in (40) and (51) have four roots since it is a quartic polynomial in v^2 . However, it is possible to reduce (64) to a problem where the denominator is a cubic polynomial, through a simple change of variable, but that is out of the scope of this discussion. Suffice to say that once this is achieved, everything previously said about (40) and its solutions may apply. In what follows, we will consider the case of physical interest where $v(0) = 0$ ($u(0) \neq 0$); i.e., when we want to generate the second harmonic starting from the fundamental. Then $\Gamma_0 = 0$ and (64), becomes

$$\xi = \pm(1/2\tilde{Q}) \int_0^{v^2} [v^2(1-v^2)^2 (1/\tilde{Q}^2 - v^2)]^{-1/2} d(v^2). \quad (65)$$

For $\tilde{Q}^2 > 1$, direct integration, after some algebra, gives

$$v^2(\xi) = 1/[\tilde{Q}^2 + (\tilde{Q}^2 - 1) \cot^2 \{(\tilde{Q}^2 - 1)^{1/2} \xi\}]. \quad (66)$$

The fundamental and second harmonic amplitudes vary periodically with ξ , with the period given by

$$\Pi_{\xi} = \pi/(\tilde{Q}^2 - 1)^{1/2}. \quad (67)$$

This indicates recurrent behavior, similar to the case of harmonic generation with quadratic nonlinearity and in the presence of dispersion. All nonlinear materials have quadratic as well as cubic nonlinearities, and the simple analysis above tells us that periodic exchange of energy will occur if the condition

$$\beta_3/2\beta_2 u(0) > 1 \quad (68)$$

is satisfied. The variation of the fundamental and second harmonic amplitudes for this case is shown in fig. 5.

On the contrary, for $\tilde{Q}^2 < 1$, direct integration of (65) gives

$$v^2(\xi) = [\tilde{Q}^2 + (1-\tilde{Q}^2)\coth^2 \{ (1-\tilde{Q}^2)^{1/2} \xi \}]. \quad (69)$$

This suggests an asymptotic increase in the second harmonic amplitude with gradual decay of the fundamental as shown in fig. 6, and is similar to the case of harmonic generation in the presence of quadratic nonlinearity and no dispersion.

4. Self-refraction

As one of the first effects of a cubic nonlinearity on wave propagation, we will first consider self-refraction of a beam. To get a physical picture, consider a beam with a Gaussian-like profile as shown in fig. 7. If the medium is cubically nonlinear, we can describe the nonlinearity in terms of n_2 , the nonlinear coefficient of the refractive index, which is related to β_3 as given in (12). If n_2 is greater than zero, regions along propagation with greater amplitude will possess a greater refractive index than a region with lower amplitudes. The result is a refractive index profile much like graded index optical fibers. If we trace 'rays', these would therefore appear to bend towards the axis of propagation, indicating a reduction of the beam waist size, and hence an increase in the on-axis amplitude. This simple picture would however suggest that the on-axis amplitude should tend to infinity; however this does not occur since diffraction puts a limit to the minimum waist size. This is shown in fig. 7. Heuristically speaking, this makes sense since the amount of diffraction (as predictable from the angle of

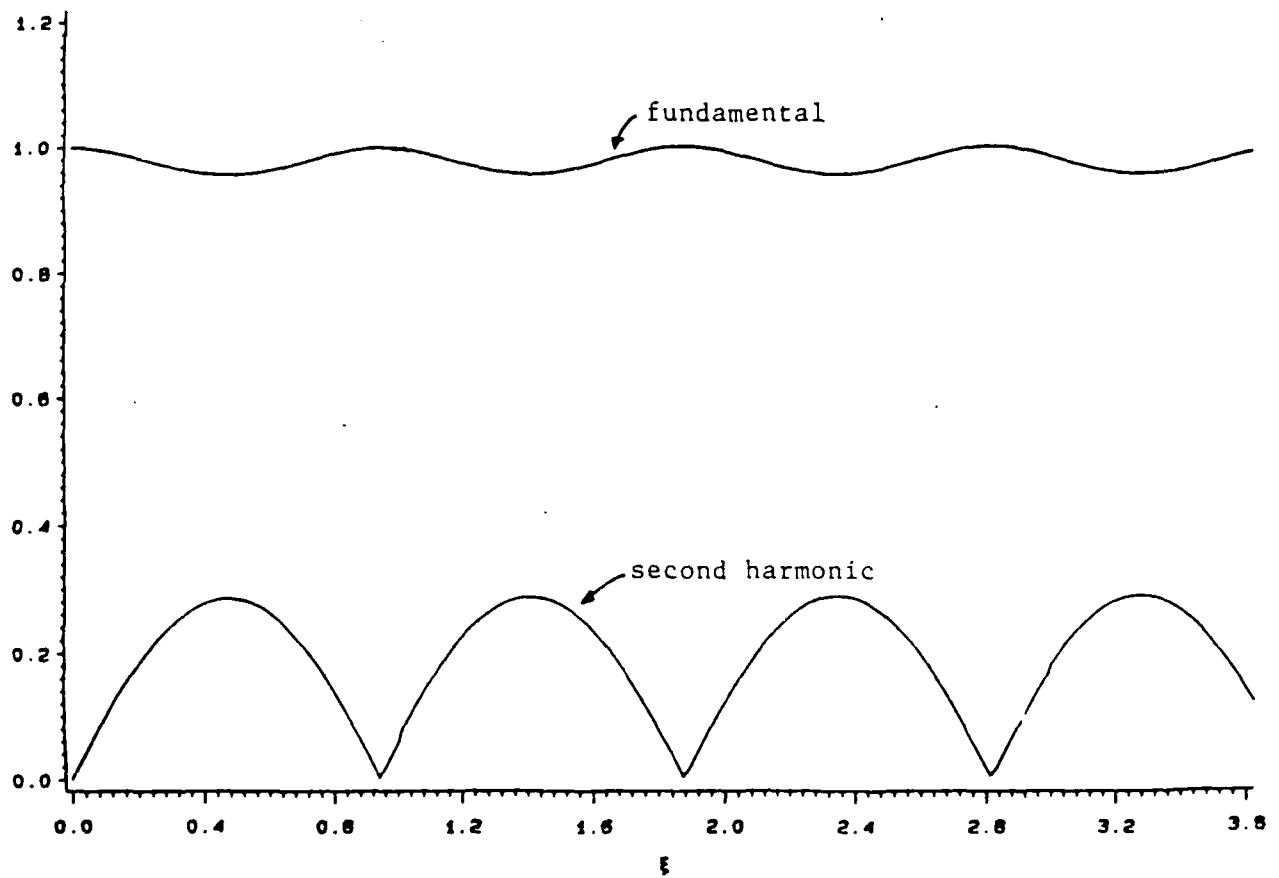


Fig. 5. Variation of the fundamental and the second harmonic with propagation in the presence of quadratic and cubic nonlinearities and no dispersion. The parameter $\tilde{Q} = 3.5$.

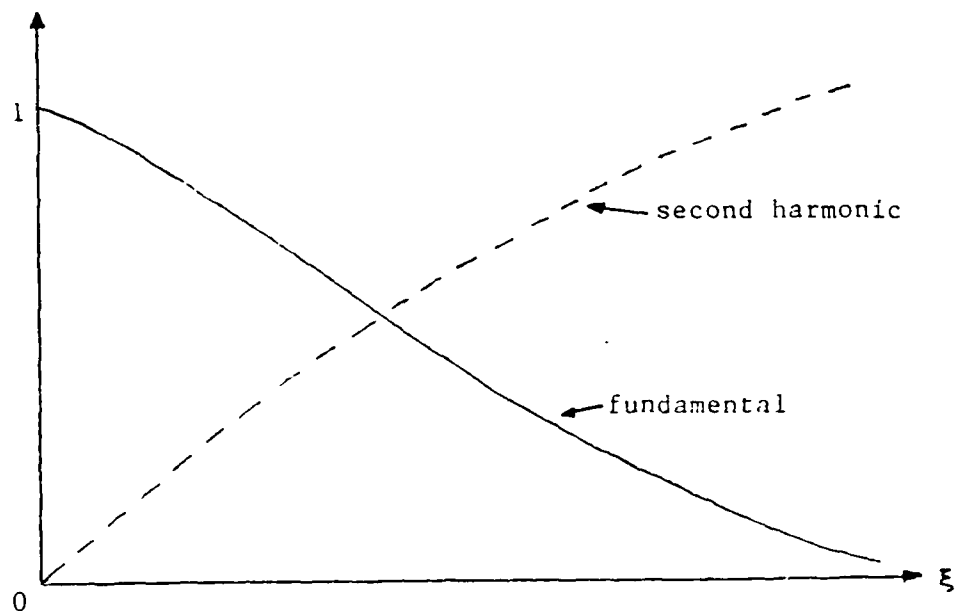
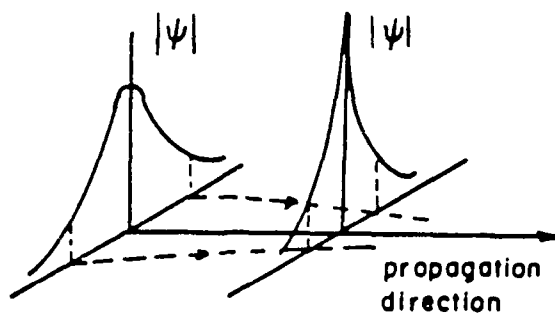
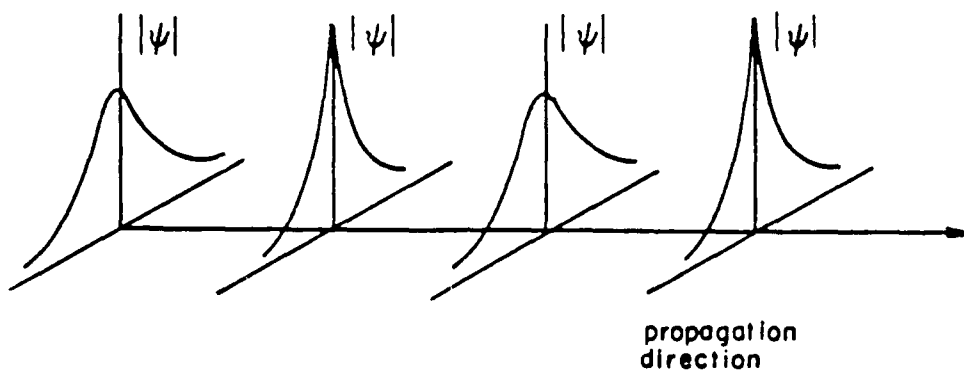


Fig. 6. Variation of the fundamental and the second harmonic with propagation in a medium with quadratic and cubic nonlinearities and no dispersion. The parameter $\bar{Q} < 1$.



(a)



(b)

Fig. 7. Self-focusing of a beam in a medium with a negative cubic nonlinearity ($\beta_3 < 0$). (a) ray trajectory: rays tend to converge toward the direction of maximum refractive index; (b) periodic focusing. This occurs since the beam waist can decrease only till the point nonlinear effects dominate over diffraction.

diffraction) depends on the ratio of the wavelength to the waist size. For an arbitrary initial beam profile, therefore, we would expect initial reduction of beam waist size before diffraction effects start to dominate and spread the beam again, resulting in periodic focussing. It turns out that while this is mostly true for a beam in a two-dimensional geometry, it may not be true for the three-dimensional case. It is also possible to find the right beam profile for which the beam-narrowing effect of nonlinearity exactly balances the beam-spreading effect of diffraction [4], [15], [16], [17]; this will be derived shortly.

For the opposite kind of nonlinearity, it is easy to argue that the beam will spread more than it does for the linear diffraction-limited case (see fig. 8).

In what follows, we will first derive an evolution equation for an arbitrary beam profile in a cubically nonlinear medium and derive an analytic expression for the diffraction-free beam in the medium. We write ψ as

$$\psi = (1/2)\psi_e(x,y,z) \exp j(\omega_0 t - k_0 z) + \text{c.c.} \quad (70)$$

and substitute in (5) with $\beta_2 = 0$ to get, after some algebra,

$$2jk_0 d\psi_e/dz = \nabla_t^2 \psi_e - (\beta_3 k_0^2/2) \psi_e^2 \psi_e^* , \quad (71)$$

where we have only retained contributions around (ω_0, k_0) . Furthermore, we have assumed $\omega_0/k_0 = c_0$ and assumed ψ_e to be a slowly varying function of z in the sense that

$$|d^2 \psi_e/dz^2| \ll k_0 |d\psi_e/dz|. \quad (72)$$

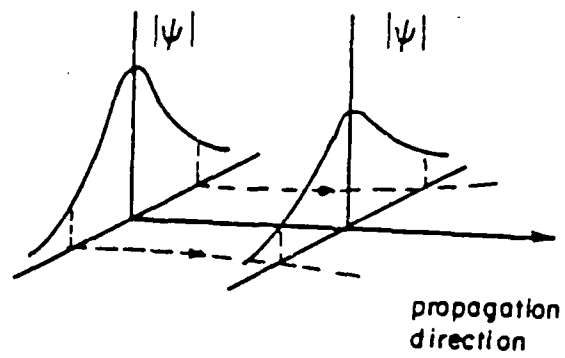


Fig. 8. Self-defocusing of a beam in a medium with a negative cubic nonlinearity. The beam spreads more than the linear diffraction-limited case.

In (71), ∇_t^2 denotes the transverse Laplacian $\partial^2/\partial x^2 + \partial^2/\partial y^2$. (71) with $\beta_3 = 0$ is identical to a PDE for ψ_e which can be readily solved using Fourier transform techniques [18] to yield the Fresnel diffraction formula [4], [19]. Thus, in (71), the first term on the RHS is due to diffraction, while the second term represents the nonlinear contribution. Eq. (71) has the same form as the nonlinear Schrodinger equation [2], [4], [17], [20], which is used to explain soliton propagation through fibers [21].

In our quest for the expression of $|\psi_e|$ that does not depend on z , we may substitute

$$\psi_e(x, y, z) = a(x, y) \exp(-jkz) \quad (73)$$

in (71) to get

$$\nabla_t^2 a = -2\kappa k_0 a + (\beta_3 k_0^2/2) a^3. \quad (74)$$

Consider, first, the case where we have one transverse direction, viz., x . Then it may be readily verified that a particular solution to (74) may be expressed in the form [22]

$$a(x) = A \operatorname{sech} Kx \quad (75)$$

where

$$A = (8\kappa/\beta_3 k_0)^{1/2}, \quad (76a)$$

$$K = 1/(-2\kappa k_0)^{1/2}. \quad (76b)$$

We note that, from above, $\kappa < 0$ and $\beta_3 < 0$ for a physical solution. Now β_3

< 0 implies $n_2 > 0$ (see (12)), which is in agreement with our heuristic description for self-focusing. A plot of the envelope is shown in fig. 9.

For two transverse directions, viz., x and y , we will only consider the case where we have radial symmetry, and express the transverse Laplacian in polar coordinates:

$$\partial^2/\partial x^2 + \partial^2/\partial y^2 = \partial^2/\partial \rho^2 + (1/\rho)\partial/\partial \rho. \quad (77)$$

Using the definitions

$$\begin{aligned} a &= (2\kappa/\beta_3 k_0)^{1/2} \bar{a} \\ \rho &= (-1/2\kappa k_0)^{1/2} \bar{\rho}, \end{aligned} \quad (78)$$

eq. (74) may be recast in the form

$$\partial^2 \bar{a}/\partial \bar{\rho}^2 + (1/\bar{\rho})\partial \bar{a}/\partial \bar{\rho} - \bar{a} + \bar{a}^3 = 0. \quad (79)$$

This equation has no analytic solutions; the solutions are thus obtained by numerical methods [2], [15], [16] and are shown in fig. 10. These are "multimodal" in nature, the mode number depending on the initial condition $\bar{a}(0)$.

An approximate solution for an arbitrary initial beam profile can be found by starting from (71), writing down the "eikonal equations" during propagation by resolving ψ_e into its amplitude and phase, and assuming power series solutions for these quantities [23]. The calculations confirm periodic behavior if we consider one transverse dimension; but are outside the scope of our discussion. We end this section by showing pictures of this periodic behavior for an initial Gaussian profile (fig. 11a) that was

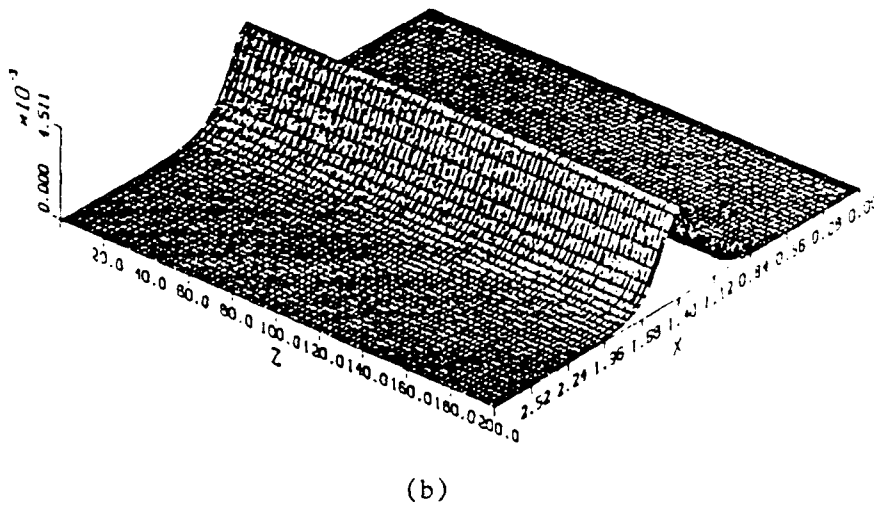
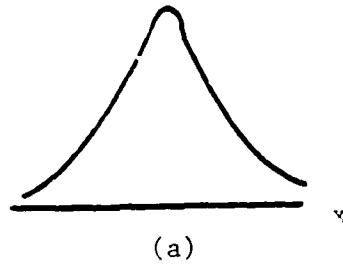


Fig. 9. Propagation of a stationary beam (a) having the form as given by eqs.(75), (76). Fig. (b) was generated by means of a split-step algorithm in which diffraction was accounted for in the spatial frequency domain and nonlinearity in the space domain. The stationary beam is a result of a delicate balance between nonlinearity and diffraction.

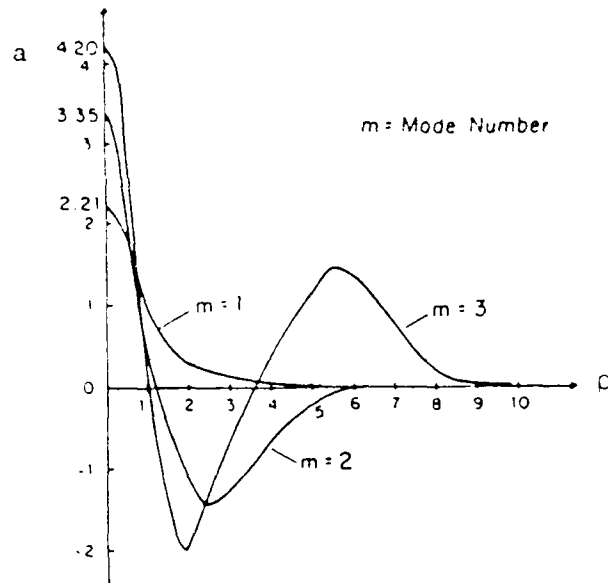
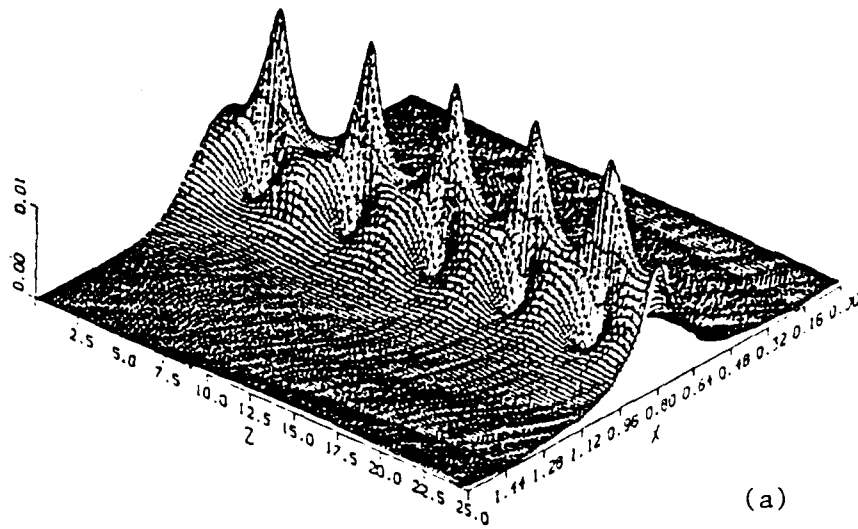
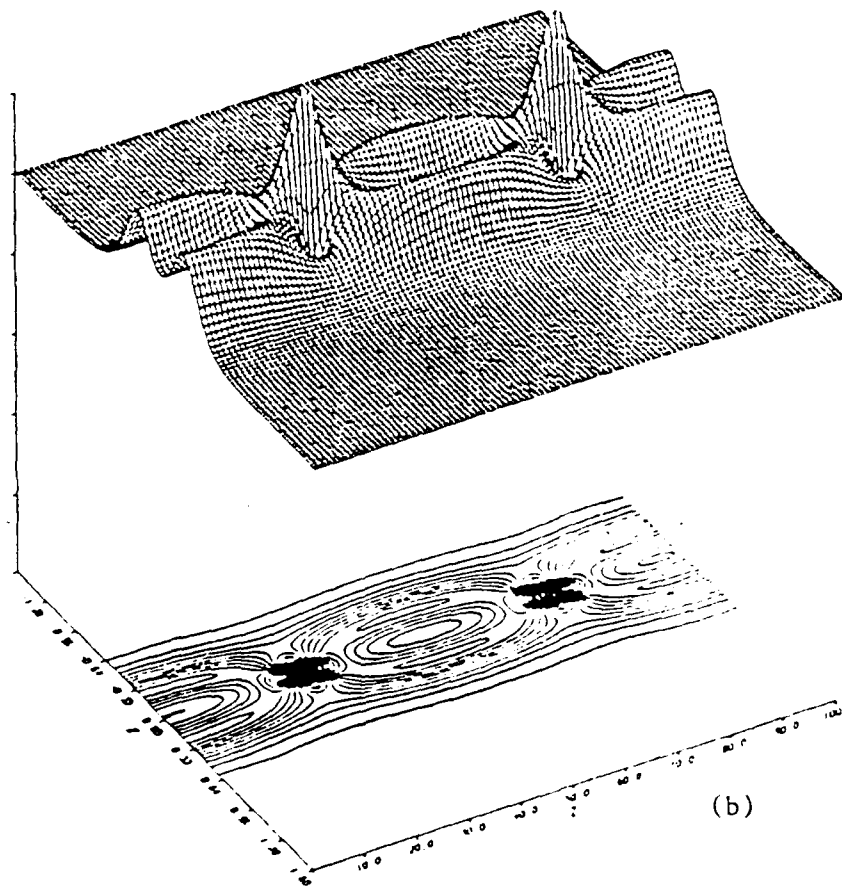


Fig. 10. Numerical solutions to eq. (79) showing amplitude profile for higher-order modes. The initial values for the respective modes as written on the figure ensure that the solution decays to zero at infinity.



(a)



(b)

Fig. 11. (a) Periodic self-focusing of an initial Gaussian profile during propagation through a self-focusing medium; (b) mutual attraction of two such beams in a self-focusing medium. The lower picture in (b) is an equiphase contour to highlight the mutual attraction.

numerically performed by employing a split-step-type angular plane wave spectrum method where diffraction is accounted for in the spatial frequency domain (recall our comment of eq. (71) for $\beta_3 = 0$ before) while the nonlinear effect is incorporated in the space domain [24]. The interaction of two beams adjacent to each other is shown in fig. 11b, which shows mutual "attraction" under the effect of nonlinearity.

5. Optical Bistability

Optical bistability refers to the existence of two stable states of an optical system for a given set of input conditions. It is interesting physically because it represents a new kind of nonlinear system in optics. Such an effect is also of obvious practical interest, as it offers a means of realizing all-optical switching for optical computers [25].

The typical characteristics of an optically bistable system are illustrated in fig. 12. A gradual increase in input power produces a steady increase in the output power or intensity until reaching a critical value where the output jumps up. On decreasing the input, the output does not immediately fall sharply but remains on the upper branch of the curve until the input is reduced to a lower critical value, at which the output jumps down again. In the region between these two critical points, there are two stable states for a given incident power. In addition to being hysteretic, the system also shows switching transitions, usually at both edges of the bistable region. Also, the state the bistable device actually assumes depends on the direction in which it traverses the hysteretic curve, i.e. it has a memory.

In general, the requirements of these bistable characteristics requires a nonlinear input/output relationship and a positive feedback. In what follows, we will first set forward an example of a hybrid bistable system e.g., an acoustooptic bistable device to point out the requirements for

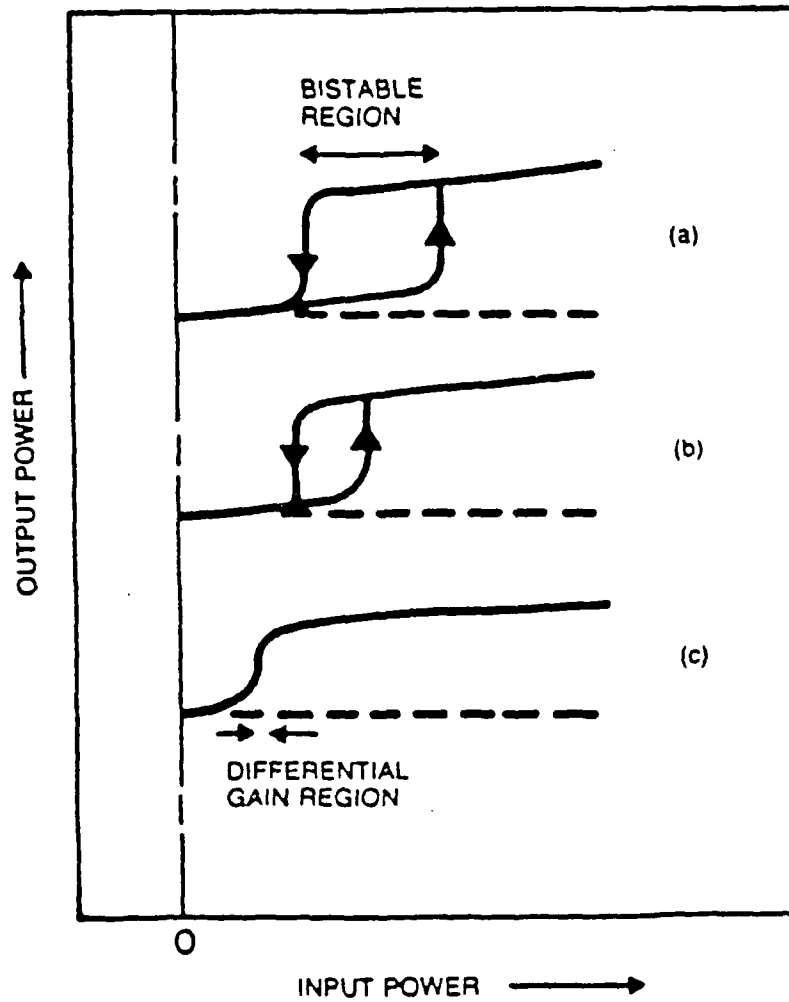


Fig. 12. Typical characteristics of an optically bistable system. As shown in the sequence of pictures, the width of the bistable region may be changed by varying the feedback parameter.

bistability mentioned above. This will be followed by examples of a nonlinear Fabri-Perot cavity and a linear nondispersive/nonlinear (dispersive) interface-type arrangement, both of which exhibit optical bistability. An excellent reference on optical bistability is the book by Gibbs [26].

5.1 Acoustooptic Bistability

If the diffracted light from an acoustooptic device operating in the Bragg regime is detected, amplified and fed back to the transducer driving the acoustooptic cell, a bistable device results. Fig 13 shows the experimental arrangement [27]. An acoustooptic cell is driven with a 40 Mhz generator which creates the acoustic grating. The first-order diffracted light from a He-Ne laser is detected and fed back to the transducer in phase with the external acoustic "input". If we denote the incident light field by ψ_{inc} , the undiffracted and diffracted light fields by ψ_0 and ψ_1 respectively, then the "output" ψ_1 is given by

$$\psi_1 = \psi_{inc} \sin (\hat{\alpha}/2), \quad (80)$$

where $\hat{\alpha}$ is the peak phase delay encountered by the light in the interaction region and is proportional to the amplitude S of the sound field. Note that $\psi_0 = \psi_{inc} \cos (\hat{\alpha}/2)$, to maintain conservation of energy. Note that the assumption made in deriving (8)) is that the sound pressure ($\propto \hat{\alpha}$) remains constant during the interaction.

If, now, the first order diffracted light intensity is detected by a photodetector and the resulting electrical signal amplified (by passing it through an amplifier with a gain constant β) and fed back to the transducer

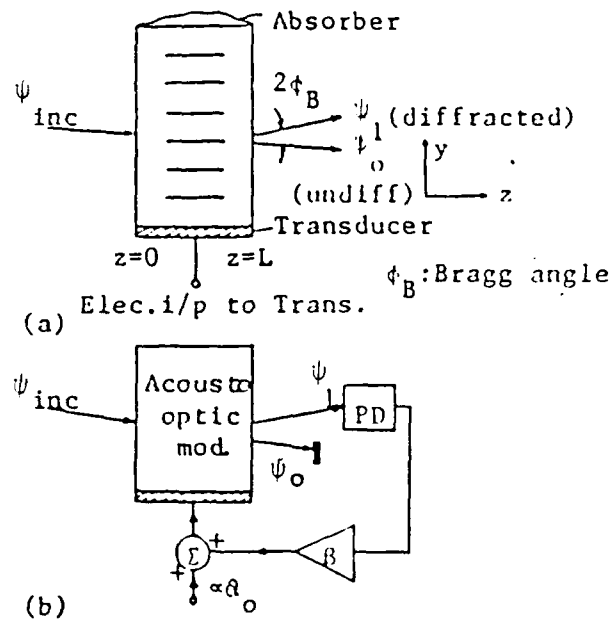


Fig. 13. (a) Acoustooptic bistable device operating in the Bragg regime;
(b) hybrid bistable device

in unison with external bias ($\hat{\alpha}_0$), we have a system with a nonlinear input ($\hat{\alpha}$) - output (ψ_1) relationship, and having a positive feedback. The effective $\hat{\alpha}$ scattering the light in the acoustooptic cell may be written as

$$\hat{\alpha} = \hat{\alpha}_0 + \tilde{\beta} |\psi_1|^2, \quad (81)$$

where $\tilde{\beta}$ denotes the product of the gain constant β of the amplifier and the conversion efficiency of the photodetector.

Note that under the feedback action, $\hat{\alpha}$ can no longer, in generality, be treated as a constant. In fact $\hat{\alpha}$ can be treated as constant during interaction iff the interaction time, given as the ratio of the laser beam width (≈ 1 mm) and the bulk speed of sound in the cell (≈ 2000 m/s), is much smaller compared to the delays incorporated by the finite response time of the photodetector, the r.f. sound cell driver and the feedback amplifier, or any other delay line that may be purposely installed (e.g., an optical fiber or coaxial cable) in the feedback path. We will consider this case only.

Based on the discussion above, we conclude that corresponding to a fixed input ($\propto \hat{\alpha}_0$), the output ψ_1 (or $|\psi_1|^2 = \psi_1^2$, if we assume ψ_1 to be real) will undergo a series of iterations at every instant $\hat{\alpha}$ is updated through the feedback action. The value of ψ_1^2 after n iterations may be written, using (80) and (81), as [28]

$$\psi_1^{2(n+1)} = \psi_{inc}^2 \sin^2 [(\hat{\alpha}_0 + \tilde{\beta} \psi_1^{2(n)})/2]. \quad (82)$$

The analysis of (82) involves a knowledge of the theory of autonomous dynamical systems of which only rather recent analysis has been performed for quadratic maps of the type

$$x_{n+1} = \mu x_n (1 - x_n), \quad (83)$$

and is out of the scope of our discussion. Suffice to state that the behavior of (83) is dynamically simple for $0 \leq \mu \leq 3$ but chaotic when $\mu \geq 4$ [28], [29]. In fact, the map undergoes a series of period-doubling bifurcations en route to chaos as the value of μ increases.

In what follows, we will discuss the steady-state behavior of (82) ($n \rightarrow \infty$) for different values of $\hat{\alpha}_0$. Rather than go through an extensive stability analysis of the steady state, we will draw the analogy between the operation of the bistable device with an electronic Schmitt trigger [30] which also exhibits hysteretic properties, and give an equivalent circuit representation. First, note from (82) that the steady state relationship reads

$$\psi_1^2 = \psi_{inc}^2 \sin^2 [(\hat{\alpha}_0 + \tilde{\beta} \psi_1^2)/2] \quad (84)$$

and is plotted in fig. 14 for different values of $\tilde{\beta}$. Note that $\tilde{\beta} = 2.2$ is the lowest admissible value of the feedback parameter to observe any hysteresis. With increase in $\tilde{\beta}$, the area under the hysteresis curve increases, and, more noticeably, the lower threshold moves to the left. This makes sense since, upon differentiating (84) w.r.t. $\hat{\alpha}_0$, we get

$$d\psi_1^2/d\hat{\alpha}_0 = (\psi_{inc}^2/2) (\sin \hat{\alpha}) / [1 - (\tilde{\beta}/2) (\sin \hat{\alpha})]; \quad (85)$$

hence $d\psi_1^2/d\hat{\alpha}_0$ will become infinite when

$$(\tilde{\beta}/2) \sin \hat{\alpha} = 1, \quad (86)$$

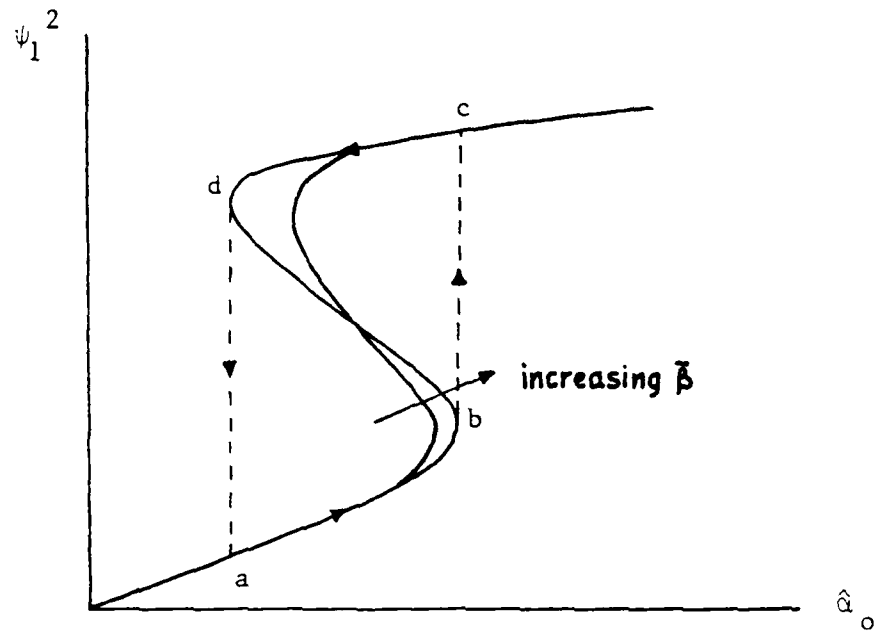


Fig. 14. Sketch of the steady-state relationship for the hybrid acoustooptic bistable device. Transitions are marked by dotted lines and path abcd completes the hysteresis cycle.

which implies $\bar{\beta} > 2$ for the onset of hysteresis.

In passing, we remark that in a practical Bragg operation, some amount of light is also diffracted into higher orders, noticeably the second order. Issues such as improvement of performance by reducing the second-order diffraction or the effect of a second-order feedback are current topics of interest. We also mention that similar hysteretic behavior may be observed by treating ψ_{inc}^2 and $\bar{\beta}$ as the inputs and treating the other variables as parameters [27].

For our configuration, the equivalent circuit in terms of an electronic Schmitt trigger is shown in fig. 15 [28]. Readers familiar with an OP-AMP realization of the Schmitt trigger may recognize that the transfer characteristic of the circuit when the loop gain is greater than 1 has a shape (see fig. 16) similar to the curves in fig. 14. The part of the curve with a negative slope is unstable, and there are two stable states. Transition from one state to the other occurs at the upper and lower thresholds of the input. The optically bistable device operates in a similar way; with transitions along the dotted lines in fig. 14.

5.2 The Nonlinear Fabri-Perot Cavity

Consider a CW laser beam injected into an optical cavity which is tuned or nearly tuned to the incident light. In general, the incident field is partly transmitted, partly reflected and partly absorbed. When the cavity contains an absorbing material resonant or nearly resonant with the incident electric field, the transmitted power becomes a nonlinear function of the incident power. The behavior of the system is determined by a parameter which depends on the unsaturated absorption coefficient of the sample per

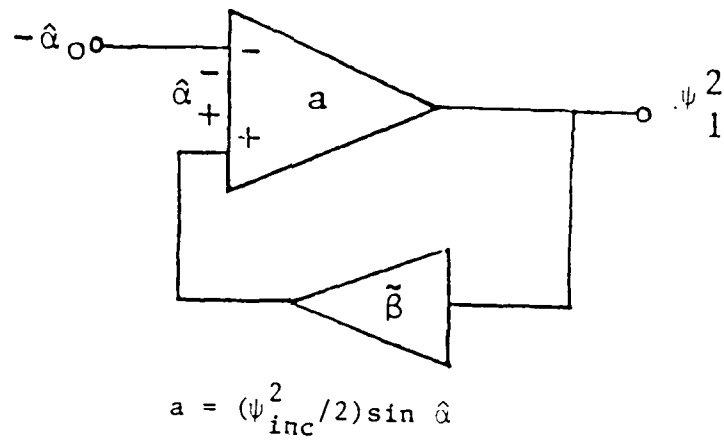


Fig. 15. Comparison of the hybrid acoustooptic device with an electronic Schmitt trigger. The small signal gain with feedback is given by eq. (85). Unlike the electronic Schmitt trigger, the gain characteristics of the amplifier do not possess a hard nonlinearity.

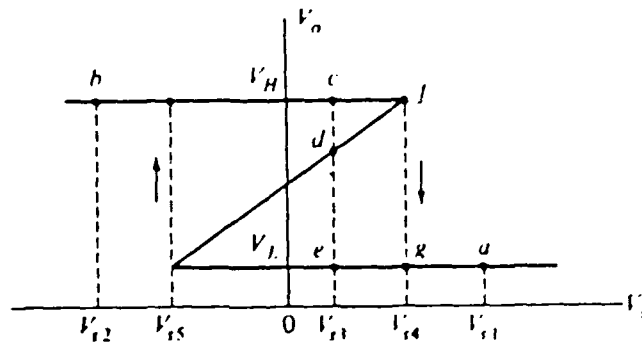


Fig. 16. Transfer characteristics of an electronic Schmitt trigger using the model of an ideal OP-AMP. V_o is the output while V_i represents the input, and should be compared to $-\hat{a}_0$ in fig. 15. Comparison with fig. 14 reveals the essential differences: (a) the curve seems reflected about a vertical line, this is due to the fact that the inputs are similar upto a negative sign, and (b) the upper and lower steady states are well-defined, due to the hard-limiter model of an ideal OP-AMP.

unit length, its length and on the mirror transmittance. If one increases the value of this parameter above a certain threshold, the steady-state input-output curve becomes S-shaped, indicating bistability and hysteresis. The threshold value depends on the cavity mistuning, the atomic detuning, the inhomogeneous linewidth and the type of cavity, to name a few. When the incident field is in perfect resonance with the atomic line so that dispersion does not play a role, we have purely absorptive bistability. On the other hand, if the atomic detuning is so large so that absorption becomes negligible, we have purely dispersive bistability [31].

In order to describe theoretically the phenomenon of bistability, we will consider a unidirectional ring cavity as shown in fig. 17. For simplicity, we assume that mirrors 3 and 4 have 100% reflectivity. We will denote the reflection and transmission coefficients of mirrors 1 and 2 as R and T respectively.

Now, the dynamics of the "active" cavity between mirrors 1 and 2 may be modelled in terms of the Maxwell-Bloch equations [26]:

$$\partial E_e / \partial t + c_0 \partial E_e / \partial z = -g P_e, \quad (87a)$$

$$\partial P_e / \partial t = (\tilde{\mu} / \hbar) E_e \tilde{D} - j \Delta P_e, \quad (87b)$$

$$\partial \tilde{D} / \partial t = (\tilde{\mu} / 2\hbar) (E_e P_e^* + E_e^* P_e) - \gamma_1 (\tilde{D} - N/2), \quad (87c)$$

where E_e and P_e are the slowly varying envelopes of the electric field and macroscopic polarization, c_0 represents the linear phase velocity, $\hbar = h/2\pi$ where h is Planck's constant and $\tilde{\mu}$ is the modulus of the dipole moment of the atoms. Furthermore, \tilde{D} is one half the difference between the populations of

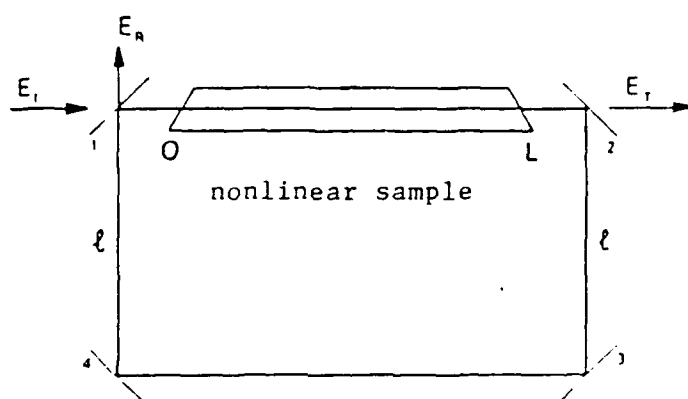


Fig. 17. The nonlinear Fabri-Perot modelled by a ring cavity. The nonlinear material is between mirrors 1 and 2. E_i , E_r and E_t denote the incident, reflected and transmitted electric fields as shown.

the lower and upper level, g is a coupling constant proportional to the frequency ω_0 of the incident field, $\Delta = (\omega_a - \omega_0) - j\gamma_2$ where ω_a is the transition frequency of the atoms and γ_1, γ_2 are the inverses of the atomic relaxation times T_1 and T_2 respectively.

In what follows, we will analyze the absorptive and dispersive cases separately. For the first, we will bring out the steady state relationship and draw the hysteresis curve to bring out the similarity (and differences) with the case considered in Section 5.1. For the second, we will get into a more detailed analysis to bring out the effects of feedback gain and the onset of instabilities.

A. Absorptive Case

Here $\omega_a = \omega_0$ so that $j\Delta$ (see (87b)) = γ_2 ; E_e, P_e may be considered real without loss of generality to simplify (87c). The coherent CW field E_{ei} enters into the cavity from the left. The cavity imposes the two following relations between E_{ei} , the transmitted field E_{et} and the fields $E_e(0,t)$ and $E_e(L,t)$ where L is the length of the atomic sample:

$$E_{et}(t) = T^{1/2} E_e(L,t),$$

$$E_e(0,t) = T^{1/2} E_{ei} + R E_e(L,t - \Delta t). \quad (88)$$

In (88), $\Delta t = (2L + L)/c_0$ is the time light takes to travel from mirror 2 to mirror 1 and

$$R + T = 1. \quad (89)$$

The second equation in (88) is a boundary condition characteristic of the ring cavity where the second term on the RHS describes a feedback mechanism so essential for bistability.

Consider the steady state $\partial E_e / \partial t = \partial P_e / \partial t = \partial \tilde{D} / \partial t = 0$. The set of equations (87) may be readily simplified to yield

$$dE_e / dz = -(\mu g N / 2 \hbar c_0 \gamma_2) E_e / [1 + E_e^2 / (\hbar^2 \gamma_1 \gamma_2 / \mu^2)]. \quad (90)$$

Eq. (90) shows how the "effective" propagation constant for the electric field, and hence, the refractive index, depends on the electric field itself, and thus brings out the physics of the nonlinearity constants viz. β_3 , χ_{1111} , n_2 and γ introduced in Section 2.

For notational convenience, we introduce the parameter

$$\alpha_c = \mu g N / 2 \hbar c_0 \gamma_2 \quad (91)$$

and a normalized field

$$\tilde{\psi}_e = \mu E_e / \hbar (\gamma_1 \gamma_2)^{1/2} \quad (92)$$

to recast (90) into

$$d\tilde{\psi}_e / dz = -\alpha_c \tilde{\psi}_e / (1 + \tilde{\psi}_e^2), \quad (93)$$

which can be easily integrated and evaluated at $z=L$. The result is

$$\ln(\tilde{\psi}_e(0) / \tilde{\psi}_e(L)) + (1/2) [\tilde{\psi}_e^2(0) - \tilde{\psi}_e^2(L)] = \alpha_c L. \quad (94)$$

Now, we define normalized incident and transmitted amplitudes as

$$\tilde{\psi}_{ei,t} = \mu E_{ei,t} / \kappa (\gamma_1 \gamma_2 T)^{1/2}. \quad (95)$$

Then (88) in the steady state transforms to

$$\begin{aligned} \tilde{\psi}_{et} &= \tilde{\psi}_e(L), \\ \tilde{\psi}_e(0) &= T\tilde{\psi}_{ei} + R\tilde{\psi}_{et}. \end{aligned} \quad (96)$$

With (96), eq. (94) may be rewritten as

$$\ln[1 + T(\tilde{\psi}_{ei}/\tilde{\psi}_{et} - 1)] + (\tilde{\psi}_{et}^2/2) \{ [1 + T(\tilde{\psi}_{ei}/\tilde{\psi}_{et} - 1)]^2 - 1 \} = \alpha_c L. \quad (97)$$

In the so-called double mean-field limit [31]

$$\alpha_c L \ll 1, \quad T \ll 1 \quad \text{with} \quad \alpha_c L / 2T = C = \text{constant}, \quad (98)$$

(97) has the form

$$\tilde{\psi}_{ei} = \tilde{\psi}_{et} + 2C\tilde{\psi}_{et} / (1 + \tilde{\psi}_{et}^2) \quad (99)$$

and is plotted in fig. 18. Note that the graph is an S-shaped curve (similar to the acoustooptic case) which leads to a hysteretic cycle.

We remark that the bistability arises from the combined action of the

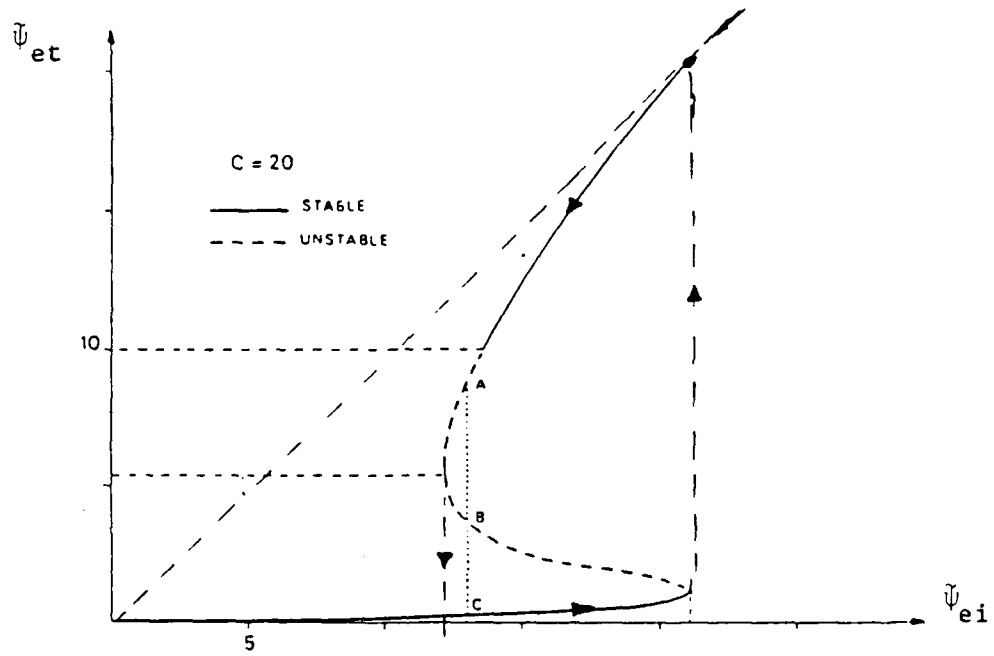


Fig. 18. Purely absorptive bistability S-curve indicating stable and unstable states and the hysteresis cycle.

nonlinear input-output relationship of the sample medium (see (94)) and the feedback of the mirrors. This feedback action is essential since it is easy to show that a plot of (97) for $T = 1$ (no reflection) does not possess the characteristic S-shape any more.

Now, introducing perturbations of the steady-state solution to the Maxwell-Bloch equations, one can perform a rigorous (although local) stability analysis for the resulting linearized system. Stability then requires that the perturbations decay exponentially in time; hence the eigenvalues of the linearized problem should have nonpositive real parts. A detailed analysis, which is done in [31], is out of the scope of this discussion.

B. Dispersive (Kerr) Case

For an analysis of Kerr-type bistability, we return to the Maxwell-Bloch equations (87) and assume $\omega_a - \omega_o \gg \gamma_2$. For a simplistic approach and to decouple the equations in the easiest possible way, we can eliminate \tilde{D} between (87b) and (87c) at around the steady states for P_e and \tilde{D} and substitute in (87a) to obtain

$$\partial \psi_e / \partial t + c_o \partial \psi_e / \partial z = j(g\mu N / \hbar |\Delta|) \psi_e - j(g\mu^3 \gamma_2 N / 2\gamma_1 \hbar^3 |\Delta|^3) \psi_e^2 \psi_e^*, \quad (100)$$

where we have written ψ_e for E_e .

It can be verified, after some algebra, that if ψ_e satisfies (100), then the total wavefunction ψ satisfies

$$\partial^2 \psi / \partial t^2 - c_o^2 \partial^2 \psi / \partial z^2 = A_1 \psi + (2\beta_3 / 3) \partial^2 \psi^3 / \partial t^2, \quad (101)$$

where

$$A_1 = -g\mu N k_0 c_0 / \hbar |\Delta|, \quad (102a)$$

$$\beta_3 = -4g\mu^3 \gamma_2 N / \gamma_1 \hbar^3 |\Delta|^3 k_0 c_0, \quad (102b)$$

if we restrict ourselves around an operating frequency ω_0 . Note (102b) shows the physics of the origin of the Kerr-type nonlinearity. Also, an inherent dispersion appears, as depicted through A_1 . In fact, the linear dispersion relation can be obtained by suppressing the nonlinear term and substituting $\psi \sim \exp j(\omega t - kz)$, and reads [2]

$$\omega^2 = c_0^2 k^2 - A_1. \quad (103)$$

Eq. (103) resembles a waveguide-like dispersion relation if $A_1 = -\omega_c^2$, where ω_c is the (linear) cutoff frequency of the waveguide. We have thus elegantly reduced the complicated Maxwell-Bloch equations to a form similar to (4b) (which was heuristically derived from a simple physical picture of phase velocity dependence on amplitudes).

We will use (101) as a model to gain insight into the instabilities encountered in the Fabri-Perot cavity with feedback, as well as to explain hysteresis and bistability for the interface problem in the next section.

In what follows, we provide a simple analysis of instantaneous optical bistability based on the model of the nonlinear medium as described above by treating it as a degenerate parametric amplifier of any noise present in the cavity. Depending upon the phase of the noise component, the net parametric round trip gain may be real and exceed unity magnitude.

Under such conditions, we expect instabilities.

From a physical point of view, the nonlinear medium acts as a degenerate traveling wave parametric amplifier for any noise in the system where the "pump", which acts as frequency $2\omega_0$, exists virtually through the action of the cubic nonlinearity on the signal itself [32]. In our quest for instabilities, we investigate if it is possible for a noise component of a certain phase to exist such that after parametric amplification in the medium and completion of its round trip through the ring cavity, this component will return in the nonlinear medium in the same phase as when it started. In cases where this is possible, we would then expect instability if the roundtrip gain exceeds unity.

An alternate way of writing (100) or (101) is to express ψ as a phasor:

$$\psi = \text{Re} \{ \psi_p \exp j\omega_0 t \}; \quad \psi_p = \psi_p(z), \quad (104)$$

where we have assumed CW propagation. Substituting this in (101) yields

$$d^2 \psi_p / dz^2 + (k_0^2 + A_1/c_0) \psi_p = (\beta_3 k_0^2 / 2) \psi_p^2 \psi_p^* \quad (105)$$

if we restrict ourselves around ω_0 and denote $k_0 = \omega_0/c_0$. Now, the total wavefunction ψ_p may be visualized as the sum of a signal and noise at the same frequency and decomposed as

$$\psi_p = \psi_{p1} + \varepsilon \psi_{p2}, \quad (106)$$

where ε is a small quantity. An order-by-order analysis of (105) after substitution of (106) gives

$$\varepsilon^0: d^2\psi_{p1}/dz^2 + (k_o^2 + A_1/c_o^2)\psi_{p1} = (\beta_3 k_o^2/2)\psi_{p1}^2\psi_{p1}^*, \quad (107a)$$

$$\varepsilon^1: d^2\psi_{p2}/dz^2 + (k_o^2 + A_1/c_o^2)\psi_{p2} = (\beta_3 k_o^2/2)(\psi_{p1}^2\psi_{p2}^* + 2\psi_{p1}\psi_{p1}^*\psi_{p2}). \quad (107b)$$

Assuming an undepleted pump ψ_{p1} , we next write, in (107a),

$$\psi_{p1} = \psi_{e1}(z) \exp(-jk_o'z) \quad (108)$$

to determine the modified propagation constant k_o' :

$$k_o'^2 = (k_o^2 + A_1/c_o^2) - (\beta_3 k_o^2/2)|\psi_{e1}|^2. \quad (109)$$

Note that the effective propagation constant is modified from k_o due to contributions from the dispersion (A_1) and the nonlinearity (β_3). Now to study the behavior of ψ_{p2} (the "noise" component), we set

$$\psi_{p2} = \psi_{e2}(z) \exp(-jk_o'z), \quad (110)$$

and substitute in (107b) to obtain

$$d\psi_{e2}/dz = j(\beta_3 k_o^2/4k_o')(\psi_{e1}\psi_{e2}^* + \psi_{e1}^*\psi_{e2})\psi_{e1}, \quad (111)$$

where we have used (109) and the "slowly varying" assumption

$$|d^2\psi_{e2}/dz^2|/|d\psi_{e2}/dz| \ll k_o' \quad (112)$$

to simplify.

In order to track the amplitude and phase of the "noise" component separately, we write

$$\psi_{e1} = a_1,$$

$$\psi_{e2} = a_2(z) \exp -j\phi_2(z), \quad (113)$$

where we have assumed the pump amplitude to be real without loss of generality. Substituting (113) in (111), we get the pair of coupled equations

$$da_2/dz = -(\beta_3 k_o^2 a_1^2 / 4k_o') a_2 \sin 2\phi_2, \quad (114a)$$

$$d\phi_2/dz = -(\beta_3 k_o^2 a_1^2 / 4k_o') (1 + \cos 2\phi_2), \quad (114b)$$

upon separating real and imaginary parts. Now (114b) may be readily integrated to give

$$\phi_2(z) = -\tan^{-1} [(\beta_3 k_o^2 a_1^2 / 2k_o') z], \quad (115)$$

where we have assumed $\phi_2(0) = 0$ for simplicity, and where k_o' is defined through (109) and (113). Substitution of (115) in (113) and integration yields, after some algebra,

$$a_2(z) = a_2(0) [1 + (\beta_3 k_o^2 a_1^2 / 2k_o')^2 z^2]^{1/2}. \quad (116)$$

With (115) and (116), we can write

$$\psi_{p2} = |\psi_{p2}(0)| [1 + (\alpha z)^2]^{1/2} \exp j(\tan^{-1} \alpha z - k'_0 z), \quad (117)$$

where

$$\alpha = \beta_3 k_0^2 |\psi_{p1}|^2 / 2k'_0. \quad (118)$$

Eq. (117) shows that the "noise" component is amplified as it travels through the nonlinear medium of length L . In fact,

$$\psi_{p2}(L) = |\psi_{p2}(0)| [1 + (\alpha L)^2]^{1/2} \exp -j(k'_0 L - \tan^{-1} \alpha L), \quad (119)$$

so that the "noise" component phasor after one round trip reads

$$\psi_{p2}(2L+2\ell) = R |\psi_{p2}(0)| [1 + (\alpha L)^2]^{1/2} \exp -j(k'_0 L + k_0(L+2\ell) - \tan^{-1} \alpha L) \quad (120)$$

where we have taken into account the phase change during propagation through the path 2341 (see fig. 17) and introduced the effects of reflection by mirrors 2 and 1.

The conditions for oscillation, or instability, (like in the acoustooptic case) demand that (a) the total round trip phase change must be an integral multiple of 2π (positive feedback), and (b) the round trip (real) gain Λ must exceed 1. The first condition, in our context, reads

$$(k'_0 L - \tan^{-1} \alpha L) + k_0(L+2\ell) = 2m\pi, \quad m \text{ integer}, \quad (121)$$

while the second condition yields

$$A = R[1 + (\alpha L)^2]^{1/2} > 1, \quad (122a)$$

implying

$$1 + (\alpha L)^2 > (1/R)^2. \quad (122b)$$

Using (121), the gain condition (122b) may be rephrased as

$$R > \cos[(k'_0 - k_0)L + 2L_0(L + \ell) - 2m\pi]. \quad (123)$$

The second term in the argument of the cosine in (123) denotes the total phase shift per round trip in the Fabri-Perot in the absence of the nonlinear sample; while the first term denotes the extra phase shift due to dispersion (A_1) and nonlinearity (β_3) in the sample. (121) and (123) should serve as good "design" equations in the construction of a Kerr-type nonlinear Fabri-Perot exhibiting bistability. Our simplified analysis is in good agreement with rigorous theories predicting bistability in such a device [33].

5.3 The Linear/Nonlinear Interface

Consider the semi-infinite linear and nonlinear regions as shown in fig. 19 with a common interface at $z = 0$. Assume, also, a plane wave incident from the linear medium to the nonlinear medium at "grazing incidence." Under the assumptions that the reflected wave is a plane wave and that the transmitted field is either a propagating plane wave or an evanescent field which decreases monotonically with distance from the interface z , but is

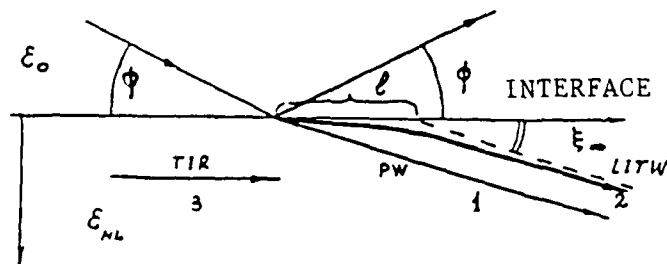


Fig. 19. Wave diagram of the nonlinear interface and for "grazing" incidence. The ray traces in the nonlinear medium (below the interface) represent (a) the traveling plane wave (PW), (b) the longitudinally inhomogeneous traveling wave (LITW) and (c) the totally internally reflected wave (TIR). The nonlinear material is assumed to possess Kerr-type nonlinearity.

independent of x and y coordinates, the scalar wave equation can be analytically solved in closed form and satisfies all the relevant boundary conditions. Solutions can be obtained for both positive and negative values of β_3 . The theory predicts hysteresis and bistability for the reflection coefficient when plotted as a function of the input amplitude, and is drawn in fig. 20 [34]. Later, numerical simulations were done to analyze the reflection of a Gaussian beam from the interface, also at grazing incidence [35], and some of the predicted effects were experimentally observed [36].

In what follows, we will consider a simpler model where a plane wave is normally incident at the interface between a linear nondispersive medium and a nonlinear dispersive medium (see fig. 21) [37]. Normal incidence makes the computations simpler, and dispersion is required to ensure bistable operation. Dispersion may be provided by having a waveguide-type structure containing the nonlinear medium. We could also think of the nonlinear medium to be excited at a frequency much different from the transition frequency of the atoms so that the material appears dispersive to the incoming field (see section 5.2).

Before proceeding with the analysis, let us remark that the linear region will be modelled by a linear wave equation of the type

$$\partial^2 \psi / \partial t^2 - c_0^2 \partial^2 \psi / \partial z^2 = 0 \quad (124)$$

and the nonlinear dispersion region by an equation similar to (101):

$$\partial^2 \psi / \partial t^2 - \tilde{c}_0^2 \partial^2 \psi / \partial z^2 = A_1 \psi + (2\beta_3/3) \partial^2 \psi^3 / \partial t^2. \quad (125)$$

We have replaced the linear phase velocity by \tilde{c}_0 in the nonlinear medium to

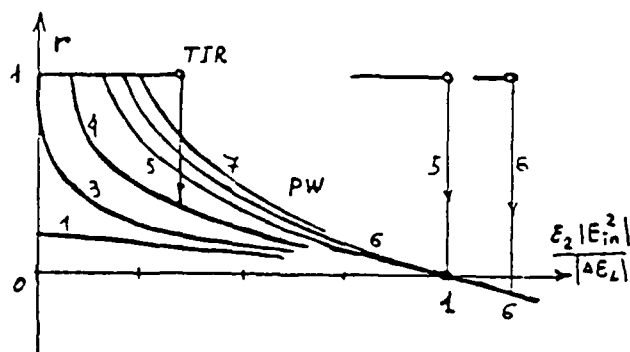


Fig. 20. Dependence of the reflectivity r on the incident light intensity $|E_{in}|^2$ at different glancing angles in the case of negative linear mismatch of susceptibilities and n_2 greater than zero. Increasing label numbers refer to decreasing ratios of the glancing angle to the critical glancing angle, which is determined from the linear mismatch of the susceptibilities.

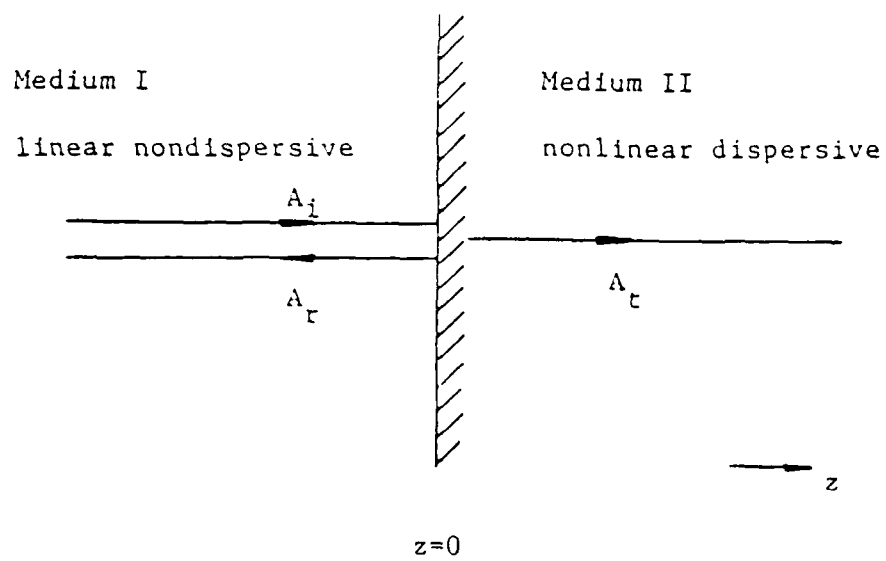


Fig. 21. Normal incidence across a linear nondispersive/ nonlinear dispersive interface.

bring out the effect(s) of linear phase velocity mismatch. A time-harmonic incident wave will be assumed, and in the propagation mode, the wave amplitude in the nonlinear medium will be determined through the amplitude transmission coefficient

$$\tau = 2\eta_o / (\eta_o + \eta'_o) = 2k'_o / (k_o + k'_o), \quad (126)$$

where k_o , k'_o refer to the propagation constants in the linear nondispersive and nonlinear dispersive regions respectively [38]. Sometimes, there is no propagation in the nonlinear region; then only evanescent modes can exist. The wave amplitude, as will be shown below, decays with distance; however, this decay is not exponential. First hand derivations will be done for this case. The output is assumed to be the amplitude of the electric field beyond a certain specific distance into the nonlinear medium. The steady state input (incident field)-output characteristics will be plotted and their stability studied to bring out the hysteretic and bistable effects.

Starting, then, from (125), and assuming a phasor form for ψ as before (see (103)), we obtain, analogous to (104),

$$d^2\psi_p/dz^2 + \tilde{k}_o^2\psi_p + (A_1/\tilde{c}_o^2)\psi_p - (\beta_3\tilde{k}_o^2/2)\psi_p^2\psi_p^* = 0, \quad \tilde{k}_o = \omega_o/\tilde{c}_o. \quad (127)$$

A particular traveling wave solution of the above has the form

$$\psi_p(z) = A_t \exp -jk_t z, \quad A_t \text{ constant} \quad (128)$$

with

$$k_t = \pm(1/\bar{\epsilon}_0) [\omega_0^2 - \omega_c^2 - (\beta_3 \omega_0^2/2) |A_t|^2]^{1/2}. \quad (129)$$

In (128), (129) the subscript 't' denotes transmission. Also, in (129), A_1 has been replaced by $-\omega_c^2$ in accordance with the discussion following eq. (103). The transmission coefficient may now be found, using (126), (129), and the fact $A_t = A_i \tau$ where A_i is the incident wave amplitude (assumed real) from the linear nondispersive region, in a transcendental form as

$$\tau = 2/[1 \pm (\bar{k}_0/k_0) \{1 - (\omega_c/\omega_0)^2 - (\beta_3/2) A_i^2 \tau^2\}^{1/2}]. \quad (130)$$

The presence of nonlinearity changes the cutoff frequency of the waveguide. To see this, note that for the condition of propagation to be satisfied the quantity in braced brackets in (130) must be greater than zero; and may be achieved with $\beta_3 < 0$ even if the linear cutoff frequency (ω_c) is greater than the operating frequency (ω_0). Under these conditions, we may say that a strong enough incident wave can "push" through a waveguide in linear cutoff. Alternatively, and in the case of our interest, there is no propagation (k_t imaginary) for $\beta_3 > 0$ ($n_2 < 0$) even for $\omega_c < \omega_0$ if the incident field is strong enough such that

$$\beta_3 A_i^2/2 > [1 - (\omega_c/\omega_0)^2]/\tau^2. \quad (131)$$

In this case it is easy to see that the "effective" cutoff frequency is increased to a value greater than the operating frequency.

While it is easier to predict the amplitude of a propagating wave in the nonlinear medium (using (130)) the evanescent solutions in the

nonpropagating case has to be determined from first principles. Since the propagating constant is now imaginary, we may write, from (129),

$$k_t(z) = -j\tilde{k}_0 [\beta_3 |A_t(z)|^2 - \{1 - (\omega_c/\omega_0)^2\}]^{1/2} \triangleq -j\delta(z). \quad (132)$$

Since A_t decays in the nonlinear dispersive medium, we may write $A_t(z+\Delta z) = A_t(z) \exp -\delta(z)\Delta z$, which, in the limit $\Delta z \rightarrow 0$, reads

$$\begin{aligned} dA_t(z)/dz &= -\delta(z)A_t(z) \\ &= -\tilde{k}_0 [\beta |A_t(z)|^2 - \gamma]^{1/2} A_t(z) \end{aligned} \quad (133a)$$

where

$$\beta \triangleq \beta_3/2; \quad \gamma = 1 - (\omega_c/\omega_0)^2. \quad (133b)$$

[It may be formally shown that $\beta, \gamma > 0$ to achieve bistability [37]; however, this is out of the scope of this rather elementary discussion].

To solve for $A_t(z)$, we first resolve it into its amplitude and phase by writing

$$A_t(z) = \tilde{A}_t(z) \exp j\phi(z). \quad (134)$$

Substitution in (133) and some algebra [37] shows that

$$\phi(z) = \phi(0) = \text{constant} ;$$

$$A_t(z) = (\gamma/\beta)^{1/2} / \sin \gamma^{1/2} [\bar{k}_0 z + (1/\gamma^{1/2}) \sin^{-1} ((\gamma/\beta)^{1/2} / \bar{A}_t(0))] . \quad (135)$$

A plot of the solution $\bar{A}_t(z)$ is shown in fig. 22. Note that $\bar{A}_t(z)$ takes on its maximum value, viz. $\bar{A}_t(0)$, at $z=0$, and decays (nonexponentially) to a critical "threshold" value $(\gamma/\beta)^{1/2}$ at

$$z = z_0 = [\pi/2 - \sin^{-1} ((\gamma/\beta)^{1/2} / \bar{A}_t(0))] / \gamma^{1/2} \bar{k}_0 . \quad (136)$$

Incidentally, $(\gamma/\beta)^{1/2}$ is the minimum value of $\bar{A}_t(z)$ for nonpropagation. It can be readily checked that

$$\psi(z,t) = (\gamma/\beta)^{1/2} \exp j\phi_0 \exp j\omega_0 t \quad (137)$$

is a solution of (127) for $z > z_0$ and the $k_t = 0$ for this case. Thus, $\bar{A}_t(z)$ decays first as in (135) till it reaches the critical value from which point it remains constant (see fig. 22).

A discussion of boundary conditions at the interface ($z=0$) for the nonpropagating case is now in order. This can be done rigorously by imposing the conditions that the wavefunctions and their spatial derivatives are continuous across the boundary. Alternatively, this can be done by realizing that eqns. (126), (130) hold at $z=0^+$. This gives

$$\bar{A}_t(0) = \{ [-\{(k_0/\bar{k}_0)^2 - \gamma\} + \{ ((k_0/\bar{k}_0)^2 - \gamma)^2 + 16A_1^2 \beta (k_0/\bar{k}_0)^2 \}^{1/2}] / 2\beta \}^{1/2} , \quad (138)$$

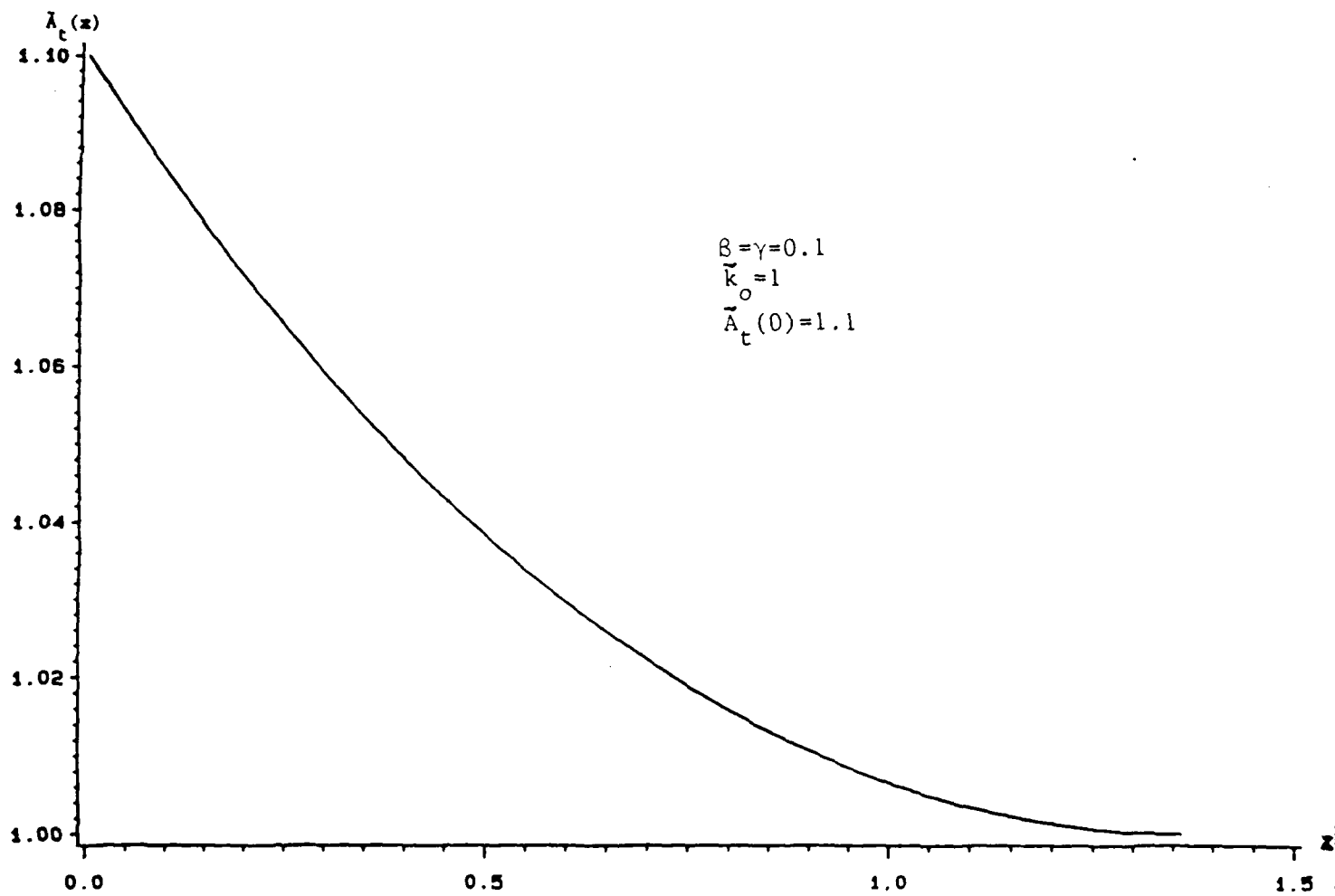


Fig. 22. Plot of the field amplitude into the nonlinear dispersive medium in the nonpropagation mode (see eq. (135)).

$$\tan \phi(0) = \{[-\{(k_o/\bar{k}_o)^2 + \gamma\} + \{((k_o/\bar{k}_o)^2 - \gamma)^2 + 16A_1^2 \beta (k_o/\bar{k}_o)^2\}^{1/2}]/2\beta\}^{1/2}. \quad (139)$$

The reflection coefficient has a magnitude 1, which is not surprising.

Now, assume the output plane to be defined as $z=z_1$ in the nonlinear medium. Fig. 23 shows the plot of $\bar{A}_t(z_1)$ vs. A_1 for a set of suitably chosen parameters β , γ , k_o , \bar{k}_o and z_1 . It comprises two main parts: the lower part (I and II) which represents the steady-state solution for the transmission case, while the upper part (III and IV) represents the solution for the nonpropagation case. Note that in the nonpropagation mode, $\bar{A}_t(z_1)$ remains constant with increase in A_1 the corresponding z_o (which depends on $\bar{A}_t(0)$, and hence on A_1) is less than z_1 . The figure is an S-shaped input/output curve which is typically associated with hysteresis and bistability. A rigorous stability analysis shows that the dotted part (region II) may correspond to an unstable steady state, resulting in bistability and hysteresis, as shown in the figure.

6. Phase Conjugation

Optical phase conjugation is a technique that employs the cubic nonlinearity effect of the optical medium to precisely reverse both the direction and the overall phase factor in an arbitrary beam of light. The process may be thought of as reflection of light from a "mirror" with unusual image-transformation properties. In order to illustrate this point, note that a conventional mirror (fig. 24a) changes the sign of the \bar{k} vector component normal to the mirror surface while leaving the tangential component unchanged. On the other hand, phase conjugation (fig. 24b) cause

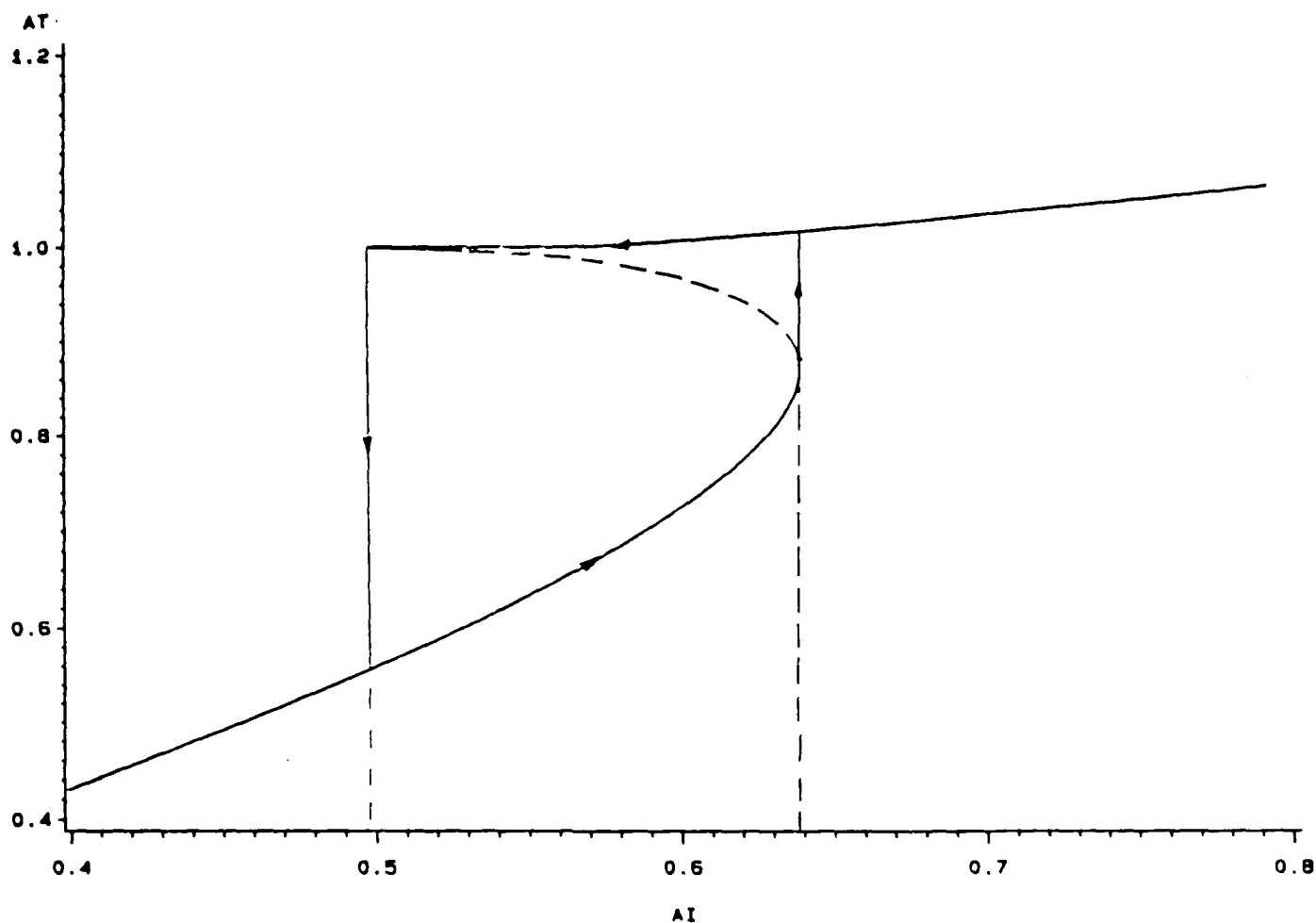


Fig. 23. Hysteresis curve for transmission across a linear nondispersive/nonlinear dispersive interface for the case of normal incidence. The nonlinearity and dispersion parameters, and the propagation constant in the nonlinear medium have exactly the same values as fig. 22; and the ratio of the (linear) propagation constants of the linear and nonlinear media is taken as $1/3$.

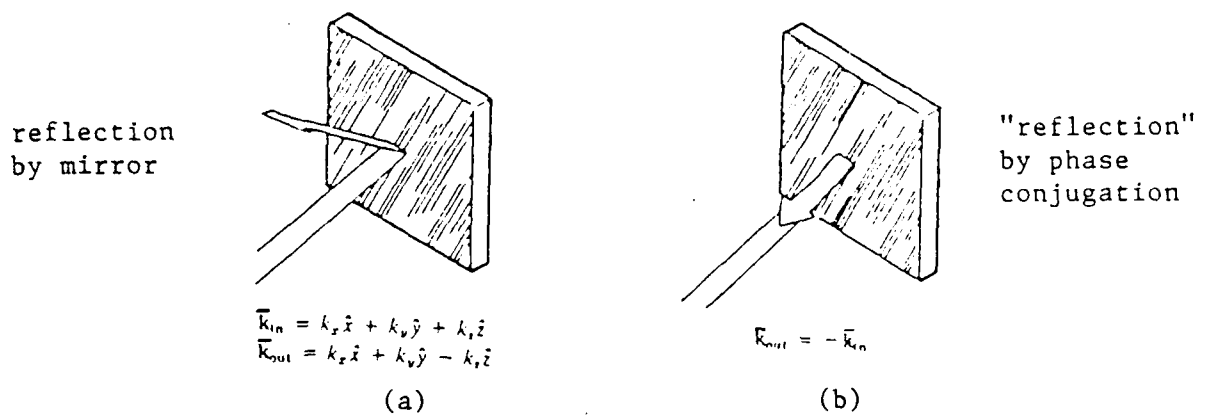


Fig. 24. Principle of phase conjugation illustrated through a comparison between conventional reflection through mirrors and reflection by phase conjugation.

an inversion of the entire vector \bar{k} , so that the incident ray exactly returns upon itself [39]. It is not hard to argue that an incident converging (diverging) beam would be conjugated into a diverging (converging) beam. Mathematically speaking, this means that if ψ_p represents the incident phasor, then ψ_p^* would represent the phase conjugated phasor.

6.1 Comparison with Holography

At this time it may be instructive to refresh our memory with the basic principles of wavefront-reconstruction imaging, or holography, first proposed by Gabor and experimentally realized by Leith and Upatneiks. The wavefront-reconstruction process consists of two basic operations: recording or information storage, and reconstruction [19]. To understand the first, consider two wavefronts, represented by their respective envelopes

$$\psi_{e1,2} = a_{1,2} \exp -j\phi_{1,2},$$

to interfere in space (see fig. 25a), resulting in an intensity

$$\begin{aligned} I &= |\psi_{e1} + \psi_{e2}|^2 \\ &= |\psi_{e1}|^2 + |\psi_{e2}|^2 + \psi_{e1}\psi_{e2}^* + \psi_{e1}^*\psi_{e2} \\ &= a_1^2 + a_2^2 + 2a_1a_2 \cos(\phi_1 - \phi_2). \end{aligned} \tag{140}$$

The intensity distribution is then usually recorded on a film and the film developed to generate a transparency or "hologram" with a transparency function that is proportional to I . To understand the reconstruction

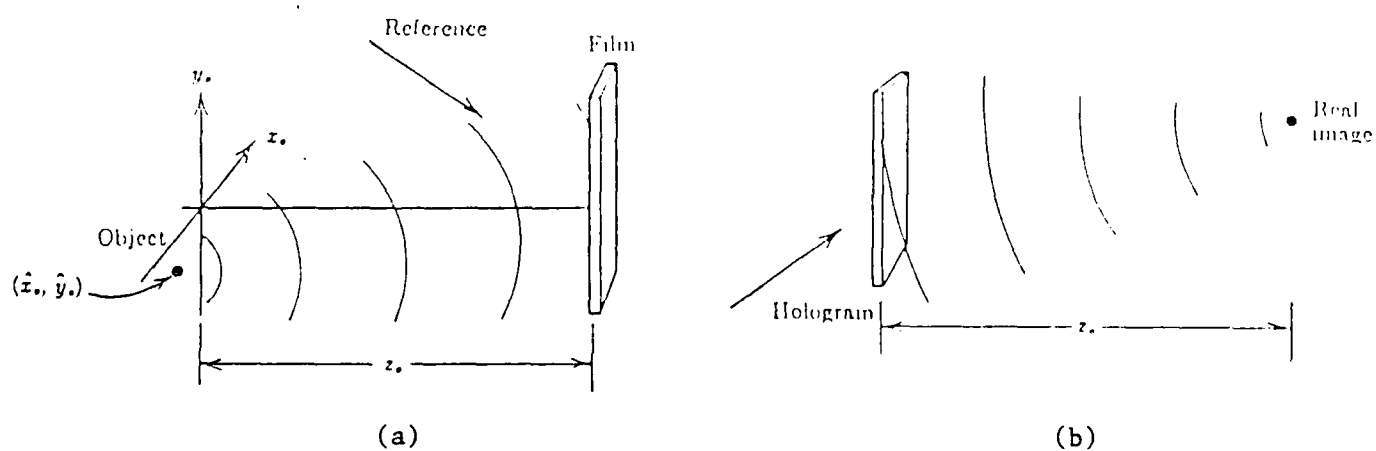


Fig. 25. Imaging by wavefront reconstruction or holography.
 (a) recording, (b) reconstruction. If the wave illuminating the hologram is proportional to the complex conjugate of the reference wave, a real image results.

process, assume that the hologram is now illuminated with a reconstruction wave ψ_{e3} . The field amplitude behind the transparency is then proportional to

$$\psi_{e3} [|\psi_{e1}|^2 + |\psi_{e2}|^2 + \psi_{e1}\psi_{e2}^* + \psi_{e1}^*\psi_{e2}].$$

Note that if ψ_{e3} is an exact duplication of one of the original waves, viz. ψ_{e2} , which we shall, from now on, call the reference wave, the third term in the above expression becomes equal to ψ_{e1} multiplied by a real term, and hence is a duplicate of ψ_{e1} , which we shall call the object wave. However, if ψ_{e3} is proportional to ψ_{e2}^* , observe that the fourth term of the above expression, which we shall name ψ_{e4} , becomes proportional to ψ_{e1}^* , and hence represents the conjugate of the object wavefront. We may state at this point that ψ_{e4} can also be thought of as being responsible for the formation of a real image of the original object (see fig. 25b) [19].

From the discussion in the last paragraph, it is clear that one can achieve phase conjugation using holographic techniques, although in the conventional sense, the process is slow, and not real-time, owing to the efforts in making the hologram. Note that in the above discussion we tacitly talked in terms of envelopes rather than phasors since reversal of the entire \bar{k} vector is not usually possible using the geometry shown in fig. 4.25. The process of introducing $\psi_{p1,2,3}$ all at once in a cubically nonlinear medium to generate ψ_{p4} speeds up the conjugation, and is technically referred to as the four-wave mixing problem. The entire \bar{k} vector of ψ_{p4} is the negative of that of ψ_{p1} . This will be discussed at some length in the following subsection.

6.2 Semiclassical Analysis

We start from eq. (5) with $\beta_2 = 0$:

$$\partial^2 \psi / \partial t^2 - c_0^2 \nabla^2 \psi = (2\beta_3/3) \partial^2 \psi^3 / \partial t^2, \quad (141)$$

and take ψ to be the sum of four waves as

$$\psi = \text{Re}[(\epsilon \psi_{p1}(z) + \psi_{p2}(y, z) + \psi_{p3}(y, z) + \epsilon \psi_{p4}(z)) \exp j\omega_0 t] \quad (142)$$

where ψ_{p2} , ψ_{p3} represent the phasors corresponding to the (undepleted) "pump" waves with ψ_{p1} , ψ_{p4} representing the "probe" and the "conjugate" wave phasors respectively. The quantity ϵ is taken to be small to emphasize that the pump energy is much larger than the probe and conjugate wave energies. Substitution of (142) into (141) and retaining only contributions around ω_0 gives the following equation upon equating coefficients of ϵ^0 :

$$\nabla^2 (\psi_{p2} + \psi_{p3}) + k_0^2 (\psi_{p2} + \psi_{p3}) = (\beta_3 k_0^2 / 2) (\psi_{p2} + \psi_{p3})^2 (\psi_{p2} + \psi_{p3}), \quad (143)$$

where $k_0 = \omega_0 / c_0$. Now, assuming the pumps to be contrapropagating in the sense that (see fig. 26)

$$\begin{aligned} \psi_{p2} &= \psi_e \exp - j(k_z z + k_y y) \\ \psi_{p3} &= \psi_e^* \exp + j(k_z z + k_y y), \quad \psi_e \text{ constant} \end{aligned} \quad (144)$$

and of equal amplitude, the following expression for the "effective"

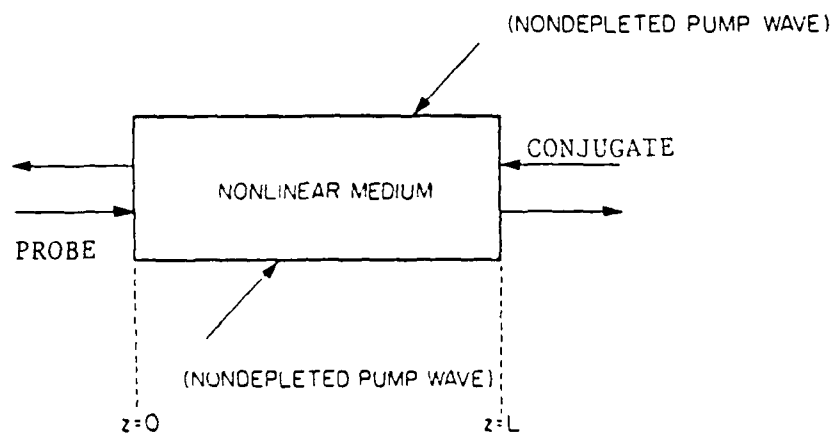


Fig. 26. Basic geometry of phase conjugation by four-wave mixing.

propagation constant k_o results upon substitution in (143):

$$k_o^2 = (k_y^2 + k_z^2) / \{1 - (3\beta_3/2) |\psi_e|^2\}. \quad (145)$$

Now equating the coefficients of ε^1 yields

$$\begin{aligned} d^2(\psi_{p1} + \psi_{p4})/dz^2 + k_o^2(\psi_{p1} + \psi_{p4}) \\ = (\beta_3 k_o^2/2) [(\psi_{p2} + \psi_{p3})^2 (\psi_{p1}^* + \psi_{p4}^*) + 2|\psi_{p2} + \psi_{p3}|^2 (\psi_{p1} + \psi_{p4})]. \end{aligned} \quad (146)$$

We now write

$$\psi_{p1} = \psi_{e1}(z) \exp - jk_o z,$$

$$\psi_{p4} = \psi_{e4}(z) \exp + jk_o z \quad (147)$$

in anticipation of a phase conjugated wave ψ_{p4} traveling in the $-z$ direction due to the probe wave ψ_{p1} (see fig. 26). We also employ the slowly-varying assumption on ψ_{e1} and ψ_{e4} . Furthermore, note that the term $(\psi_{p2} + \psi_{p3})^2$ ($= |\psi_{p2} + \psi_{p3}|^2$ for our case) defines essentially a sinusoidal phase grating in space due to the cubic nonlinearity. In the direction of propagation of the probe and the conjugate wave, however, only the term from the above expression that is spatially constant will affect their evolution. The spatial distribution of the induced phase grating will have variations along the directions of propagation of the pumps; however, these will not affect the probe and conjugate. Mathematically, this amounts to picking out the constant term from $(\psi_{p2} + \psi_{p3})^2$. Eq. (146) thus gives the following set

of coupled equations between ψ_{e1} and ψ_{e4}^* :

$$d\psi_{e1}/dz = 2j\beta_3 k_o |\psi_e|^2 (2\psi_{e1} + \psi_{e4}^*) \quad (148a)$$

$$d\psi_{e4}^*/dz = -2j\beta_3 k_o |\psi_e|^2 (\psi_{e1} + 2\psi_{e4}^*). \quad (148b)$$

To solve the system (148), we introduce

$$\tilde{\psi}_{e1} = \psi_{e1} \exp -4j\beta_3 k_o |\psi_e|^2 z$$

$$\tilde{\psi}_{e4} = \psi_{e4} \exp 4j\beta_3 k_o |\psi_e|^2 z \quad (149)$$

to recast the system in the form

$$d\tilde{\psi}_{e1}/dz = j\tilde{\delta}\tilde{\psi}_{e4}^*,$$

$$d\tilde{\psi}_{e4}^*/dz = -j\tilde{\delta}\tilde{\psi}_{e1}, \quad (150)$$

where

$$\tilde{\delta} = 2\beta_3 k_o |\psi_e|^2. \quad (151)$$

The solution to (150) for initial conditions $\tilde{\psi}_{e1}(0)$ and $\tilde{\psi}_{e4}(L)$ is given by [40]

$$\begin{aligned}\tilde{\Psi}_{e1}(z) = & j[|\tilde{\delta}| \sin(|\tilde{\delta}|z)/\tilde{\delta} \cos(|\tilde{\delta}|L)]\tilde{\Psi}_{e4}^*(L) \\ & + [\cos(|\tilde{\delta}|(z-L))/\cos(|\tilde{\delta}|L)]\tilde{\Psi}_{e1}(0),\end{aligned}\quad (152)$$

$$\begin{aligned}\tilde{\Psi}_{e4}(z) = & [\cos(|\tilde{\delta}|z)/\cos(|\tilde{\delta}|L)]\tilde{\Psi}_{e4}(L) \\ & - j[|\tilde{\delta}| \sin(|\tilde{\delta}|(z-L))/\tilde{\delta} \cos(|\tilde{\delta}|L)]\tilde{\Psi}_{e1}^*(0).\end{aligned}\quad (153)$$

In the practical case of phase conjugation, $\tilde{\Psi}_{e1}(0)$ is finite, whereas $\tilde{\Psi}_{e4}(L) = 0$. In this case, the nonlinearly reflected wave at the input plane ($z=0$) is

$$\tilde{\Psi}_{e4}(0) = j[(\tilde{\delta}/|\tilde{\delta}|)\tan(|\tilde{\delta}|L)]\tilde{\Psi}_{e1}^*(0), \quad (154)$$

where $\tilde{\delta}$ is defined in (151). Note that $\tilde{\Psi}_{e4}$ is proportional to the complex conjugate of $\tilde{\Psi}_{e1}$, as expected.

7. The Nonlinear Schrodinger Equation and Soliton Propagation

It is well known in the theory of nonlinear waves that pulses traveling in nonlinear medium distort under the effect of nonlinearity [1], [2]. Furthermore, from linear theory, we may also recall that pulses distort and spread due to dispersion in the medium [4]. It is sometimes possible, in a nonlinear dispersive environment, to ensure distortionless propagation of pulses as a result of a balance between the nonlinearity and dispersion. For baseband propagation, it is a little easier to see why this should happen: the steepening effect of nonlinearity (see fig. 1) may be balanced by the spreading, or "smoothing" effect of dispersion. For modulated pulses, both

nonlinearity and dispersion cause a chirping in frequency to develop during propagation, as well as other distortions of the envelope. Given the right amounts of nonlinearity and dispersion, it is possible, onece again, to offset the effect (s) of one with that of the other to ensure distortionless propagation of the modulated pulse [2].

In keeping with the nature of the presentation thus far, we will derive the PDE for the envelope in the nonlinear dispersive medium in the fastest possible way. Consider, first, a linear medium with arbitrary dispersion, as shown in fig. 27. Since we are discussing the behavior of modulated pulses, it is probably best to locate ourselves at a point (ω_0, k_0) of the dispersion curve (the coordinates corresponding to the carrier frequency and propagation constant) and define "excursions" around that value by a Taylor series expansion of the form [2], [4], [41]

$$\omega - \omega_0 = u_0 (k - k_0) + (u'_0/2)^2, \quad \omega > 0. \quad (155)$$

In (155), $u_0 = \partial\omega/\partial k|_{\omega_0}$ and $u'_0 = \partial^2\omega/\partial k^2|_{\omega_0}$ are called the group velocity and group velocity dispersion terms respectively, and can be explicitly calculated from a knowledge of the explicit equation describing the dispersion curve in fig. 27. Changing to variables

$$\Omega = \omega - \omega_0, \quad K = k - k_0 \quad (156)$$

we can reformulate the nature of the dispersion around the carrier frequency ω_0 as

$$\Omega = u_0 K + (u'_0/2)K^2. \quad (157)$$

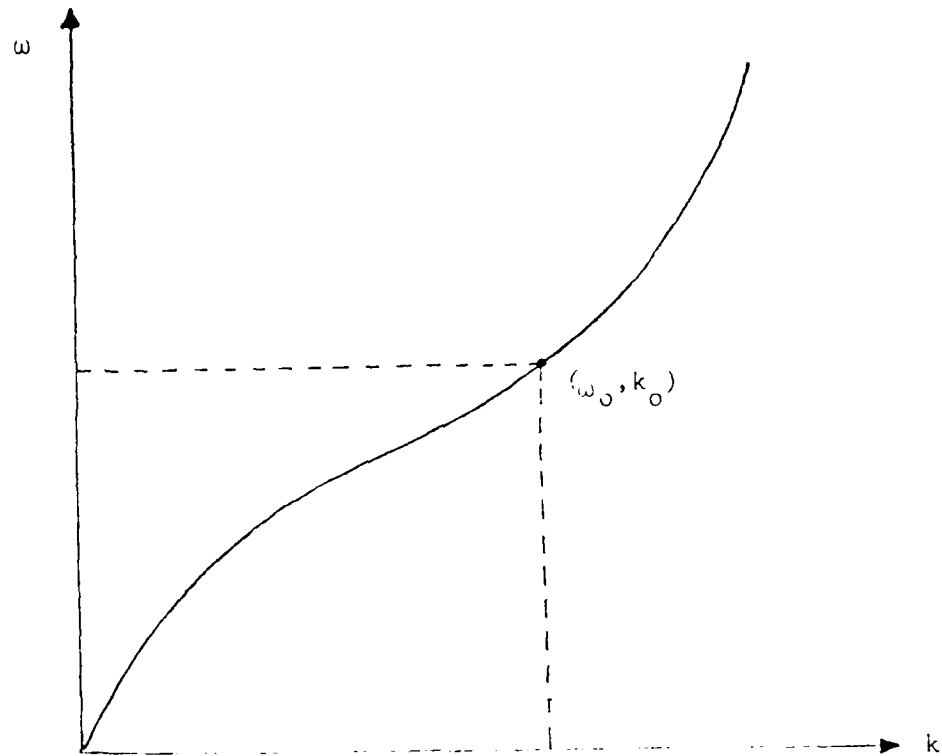


Fig. 27. Arbitrary dispersion curve showing the variation of the angular frequency ω_0 with the propagation constant k_0 .

How do we figure out the PDE describing envelope propagation ? The procedure to be followed is the inverse of what we did to calculate the dispersion relation (103) from the linear part of (101). Note in that case, we substituted $\psi \sim \exp j(\omega t - kz)$ in the linear PDE, which, in reality, amounted to replacing $\partial/\partial t$ by $j\omega$ and $\partial/\partial z$ by $-jk$, where ω and k were the respective frequency and propagation constant parameters. In this case, we do exactly the inverse: we replace Ω by $-j\partial/\partial t$ and K by $j\partial/\partial z$. The wavefunction these operators must operate on is, however, the envelope ψ_e of ψ ; since we are located around the carrier frequency on the dispersion curve. With all this, (157) yields the linear PDE [2]

$$j(\partial\psi_e/\partial t + u_0\partial\psi_e/\partial z) - (u'_0/2) \partial^2\psi_e/\partial z^2 = 0, \quad (157a)$$

or

$$j\partial\psi_e/\partial t' - (u'_0/2) \partial^2\psi_e/\partial z'^2 = 0 \quad (157b)$$

if we are in a traveling frame of reference

$$z' = z - u_0 t; \quad t' = t. \quad (158)$$

In what follows, we will modify (157) by heuristically incorporating the effects of nonlinearity. Assuming a cubic nonlinearity ($\beta_3 \neq 0$; $\beta_2 = 0$) and $\psi = \text{Re} \{ \psi_e(z, t) \exp j(\omega_0 t - k_0 z) \}$ in (3b), and using the "slowly-varying envelope" approximation, it follows that ψ_e evolves according to

$$j\partial\psi_e/\partial t' + (\omega_0\beta_3/4)\psi_e^2\psi_e^* = 0 \quad (159)$$

in a suitable traveling frame of reference. In our heuristic approach, we will include the effects of nonlinearity in (157) by simply replacing the $j\partial\psi_e/\partial t'$ in (157b) by $j\partial\psi_e/\partial t' + (\omega_0\beta_3/4)\psi_e^2\psi_e^*$. This yields

$$j\partial\psi_e/\partial t' - (u_0'/2)\partial^2\psi_e/\partial z'^2 + (\omega_0\beta_3/4)\psi_e^2\psi_e^* = 0, \quad (160)$$

which is the nonlinear Schrodinger (NLS) equation describing envelope propagation in a (cubically) nonlinear, dispersive medium [2], [4], [17], [20], [41]. The equation has been extensively used to model waves in plasma [42], water waves [43], electron and ion cyclotron waves [44] and, with minor changes of the independent variables, pulse propagation through a single mode nonlinear optical fiber [4]. We remark that the nonlinearities in fibers may be Kerr-type, while the dispersion is essentially material dispersion, since no modal dispersion effects exist.

To find particular solutions of the NLS equation, note that it has the same form as eq (71) that describes beam propagation through a cubically nonlinear medium. In fact, an interesting analogy of pulse propagation in one dimension and beam propagation may be made by comparing eqns. (160) and (71); in fact, diffraction may be looked upon as being somewhat like dispersion in space. The (real) amplitude of a particular solution is therefore of the same form as (75) and a plot appears in fig. 9, with renamed coordinates. Let us conclude by saying that solitons, as these envelope profiles are called, have been generated and propagated over long-distances through optical fibers [21], leaving open the door for innovative communication systems that can be much faster than the present ones that suffer the effects of material dispersion. The advantages of solitons are

that they not only remain undistorted by themselves in a nonlinear dispersive medium, but can also interact with each other without a change in shape [20].

8. Conclusion

This report reflects some of the work done or being done in the area of nonlinear optics. As stated in the Introduction, it is by no means complete or exhaustive, nevertheless, I hope it will get readers started in the seemingly complex though very interesting area. Since only principles have been discussed and in fair generality, the discussion could find some use in other fields, e.g., hydrodynamics and plasmas, where similar effects may be observed or, or least, simulated. References are, by no means exhaustive, rather, they have been kept at a minimum; however, interested readers can cross-reference from the cited work. It would be true to say that being a starter in the area, I could appreciate the difficulties one could incur, and the discussion presented above is just a summary of my lines of thought.

Acknowledgments

The author would like to thank Dr. Brain Henrickson of the Rome Air Development Center for suggesting and supporting this seemingly monumental task. I am grateful to Dr. Willy Hereman of the University of Wisconsin for the endless hours of cutting, pasting and analyzing on the topic of bistability. I should also acknowledge the help from my graduate students Mokhtar Maghraoui, Wonha Choe and Guanghui Cao in unifying the descriptions of optical nonlinearities, predicting harmonic generation with quadratic and cubic nonlinearities and for predicting bistability during transmission through a linear nondispersive/nonlinear dispersive interface respectively. Finally I would like to thank Bert Fancher for mastering the EGG software and her efficient typing of the manuscript.

References

1. G. B. Whitham, Linear and Nonlinear Waves. New York: Wiley, 1974.
2. A. Korpel and P.P. Banerjee, "A Heuristic Guide to Nonlinear Dispersive Wave Equations and Soliton-type Solutions," Proc. IEEE, vol. 72, pp.1109-1130, 1984.
3. A. Yariv and P. Yeh, Optical Waves in Crystals. New York: Wiley, 1984.
4. H. A. Haus, Waves and Fields in Optoelectronics. Englewood Cliffs, N.J.: Prentice-Hall, 1984.
5. A. Yariv, Quantum Electronics. New York: Wiley, 1975.
6. O. M. Phillips, "Wave Interactions," in Nonlinear Waves, S. Leibovich and A. R. Seebass, eds. Ithaca, NY: Cornell University Press, 1974.
7. N. Bloembergen, Nonlinear Optics, New York: Benjamin, 1965.
8. P. P. Banerjee and W. Choe, "Second Harmonic/Subharmonic Generation in a Medium with Quadratic and Cubic Nonlinearities," Opt. Soc. Amer. Meeting, Santa Clara, 1988.
9. E. Fermi, J. Pasta and S. Ulam, "Studies of Nonlinear Problems I," Los Alamos Rep. LA 1940, 1955.
10. L. F. McGoldrick, "Resonant Interactions among Capillary-gravity Waves," J. Fluid Mech., vol. 21, pp. 305-331, 1965.
11. P. P. Banerjee, "Subharmonic Generation by Resonant Three-wave Interaction of Deep-water Capillary Waves," Phys. Fluids, vol. 25, pp.1938-1943, 1982.
12. A. Korpel, "A Frequency Approach to Nonlinear Dispersive Waves," J. Acoust. Soc. Amer., vol. 67, pp. 1954-1958, 1980.
13. P. P. Banerjee and A. Korpel, "Stability of Acoustic Nonlinear Dispersive Eigenmodes," J. Acoust. Soc. Amer., vol. 70, pp. 157-164, 1981.
14. M. Abramowitz and I. Stegun, Handbook of Mathematical Functions New York: Dover, 1965.
15. R. Y. Chiao, E. Garmire and C. H. Townes, "Self-Trapping of Optical Beams," Phys. Rev. Lett., vol. 13, pp. 479-482, 1964.
16. H. A. Haus, "Higher Order Trapped Light Beam Solutions," Appl. Phys. Lett., vol. 8, pp. 128-129, 1966.
17. S. A. Akhmanov, A. P. Sukhorukov and R. V. Khokhlov, "Self-focussing and Self-trapping of Intense Laser Beams in a Nonlinear Medium" Sov. Phys. - JETP, vol. 23, pp. 1025-1033, 1966.

18. P. P. Banerjee, "A Simple Derivation of the Fresnel Diffraction Formula," *Proc. IEEE*, vol. 73, pp. 1959-1960, 1985.
19. J. W. Goodman, *Introduction to Fourier Optics*. New York: McGraw-Hill, 1968.
20. R. K. Dodd, J. C. Eilbeck, J. Gibbon and H. Morris, *Solitons and Nonlinear Wave Equations*. New York: Academic Press, 1982.
21. L. F. Mollenauer and R. H. Stolen, "Solitons in Optical Fibers," *Fiberopt. Technol.*, pp. 193-196, 1982.
22. A. Korpel, "Solitary Wave Formation through m-th Order Parametric Interaction," *Proc. IEEE*, vol. 67, pp. 1442-1443, 1979.
23. P. P. Banerjee, A. Korpel and K. E. Lonngren, "Self-refraction of Nonlinear Capillary-gravity Waves," *Phys. Fluids*, vol. 26, pp. 2393-2398, 1983.
24. A. Korpel, K. E. Lonngren, P. P. Banerjee, H. K. Sim and M. R. Chatterjee, "Split-step-type Angular Plane-wave Propagation," *Journal Opt. Soc. Amer. B*, vol. 3, pp. 885-890, 1986.
25. P. W. Smith and W. J. Tomlinson, "Bistable Optical Devices Promise Subpicosecond Switching," *IEEE Spectrum*, vol. 18, pp. 26-33, 1981.
26. H. M. Gibbs, *Optical Bistability: Controlling Light with Light*. New York: Academic, 1985.
27. J. Chrostowski and C. Desisle, "Acoustooptic Bistable Generator," *J. Opt. Soc. Amer.*, vol. 72, pp. 1770-1775, 1982.
28. P. P. Banerjee and T-C Poon, "Simulations of Bistability and Chaos in Acoustooptic Devices," *Proc. Midwest Symp. Circuits and Systems*. Amsterdam: North-Holland, 1987.
29. R. L. Devaney, *An Introduction to Chaotic Dynamical Systems*, Menlo Park: Benjamin/Cummings, 1986.
30. H. Taub and D. Schilling, *Digital Integrated Electronics*. New York: McGraw Hill, 1977.
31. L. Lugiato, "Theory of Optical Bistability" in *Progress in Optics* vol. 21, ed. E. Wolf. Amsterdam: North Holland, 1984.
32. A. Korpel, "Interpretation of Optical Bistability through Self-Degenerate Amplification," *Opt. Comm.*, vol. 61, pp. 66-70, 1987.
33. K. Ikeda, "Chaos and Optical Bistability" in *Coherence and Quantum Optics V*, eds. L. Mandel and E. Wolf. New York: Plenum, 1984.
34. A. E. Kaplan, "Theory of Plane Wave Reflection and Refraction by the Nonlinear Interface" in *Optical Bistability*, eds. C. M. Bowden, M. Ciftan and H. R. Robl. New York: Plenum, 1981.

35. W. J. Tomlinson, J. P. Gordon, P. W. Smith and A. E. Kaplan, "Reflection of a Gaussian Beam at a Nonlinear Interface," Appl. Optics vol. 21, pp. 2041-2051, 1982.
36. P. W. Smith and W. J. Tomlinson, "Optical Properties of Nonlinear Interfaces" in Optical Bistability, eds. C. M. Bowden, M. Ciftan and H. R. Robl. New York: Plenum, 1981.
37. G. Cao and P. P. Banerjee, "Theory of Hysteresis and Bistability during Transmission through a Linear Nondispersive-Nonlinear Dispersive Interface," to appear in J. Opt. Soc. Amer. B., January 1989.
38. R. F. Harrington, Time-Harmonic Electromagnetic Fields. New York: McGraw Hill, 1961.
39. A. Yariv and R. A. Fisher, in Optical Phase Conjugation ed. R. A. Fisher. New York: Academic, 1983.
40. D. M. Pepper and A. Yariv, "Optical Phase Conjugation using Three-wave and Four-wave Mixing via Elastic Photon Scattering in Transparent Media," in Optical Phase Conjugation ed. R. A. Fisher. New York: Academic, 1983.
41. V. I. Karpman, Nonlinear Waves in Dispersive Media. New York: Pergamon, 1975.
42. J. Tanuiti and H. Washimi, "Self-trapping and Instability of Hydrodynamic Waves along the Magnetic Field of a Cold Plasma," Phys. Rev. Lett., vol. 21, pp. 209-212, 1968.
43. V. D. Djordjevic and L. G. Redekopp, "On Two-dimensional Packets of Capillary-gravity Waves," J. Fluid Mech., vol. 79, pp. 703-714, 1977.
44. A. Hasegawa, Plasma Instabilities and Nonlinear Effects. Berlin: Springer-Verlag, 1975.



MISSION of Rome Air Development Center

RADC plans and executes research, development, test and selected acquisition programs in support of Command, Control, Communications and Intelligence (C³I) activities. Technical and engineering support within areas of competence is provided to ESD Program Offices (POs) and other ESD elements to perform effective acquisition of C³I systems. The areas of technical competence include communications, command and control, battle management information processing, surveillance sensors, intelligence data collection and handling, solid state sciences, electromagnetics, and propagation, and electronic reliability/maintainability and compatibility.